Echocardiographic Assessment of Myocardial Mechanics: Velocity, Strain, Strain Rate and Torsion

12

Hoorak Poorzand, Anita Sadeghpour, Azin Alizadehasl, and Samir Saha

Abstract

Echocardiography has been routinely used for assessment of cardiac mechanics. M-Mode and two dimensional echocardiography provide semi-quantitative data in the context of ventricular function and have limited ability in defining subtle changes in the function. Doppler tissue imaging (DTI) and Speckle tracking echocardiography (STE), two newer techniques, have emerged greater concerns for their role in quantification of ventricular systolic and diastolic function. These methods are more objective and provide more reproducible results. This chapter focuses on the technical properties of DTI, STE and tortional parameters and their clinical implication.

Keywords

Tissue Doppler imaging · Ventricular mechanics · Atrial mechanics · Strain · Velocity · Torsion

Abbreviations

2D   Two-dimensional
3D   Three-dimensional
DT   Doppler tissue
DTI   Doppler tissue imaging

ET   Ejection time
GCS   Global circumferential strain
GLS   Global longitudinal strain
GRS   Global radial strain
IVA   Isovolumic acceleration
IVCT   Isovolumic contraction time
IVRT   Isovolumic relaxation time
MPI   Myocardial performance index
ROI   Region of interest
RV   Right ventricular
SR   Strain rate
STE   Speckle-tracking echocardiography

H. Poorzand, MD, FASE
Cardiovascular Department, Faculty of Medicine, Imam Reza Hospital, Mashhad University of Medical Sciences, Mashhad, Iran

A. Sadeghpour, MD, FACC, FASE (✉)
Professor of Cardiology, Echocardiography Research Center, Rajaie Cardiovascular Medical and Research Center, Iran University of Medical Science, Tehran, Iran

A. Alizadehasl, MD, FACC, FASE
Associate Professor of Cardiology, Echocardiologist, Echocardiography and Cardiogenetic Research Centers, Cardio-Oncology Department, Rajaie Cardiovascular Medical and Research Center, Tehran, Iran

S. Saha
Cardiac Imaging Lab, Sundsvall, Sweden

Introduction

Myocardial tissue imaging and Speckle tracking have been introduced as methods to study global and regional systolic and diastolic (left and right) ventricular and atrial function. The first report appeared in 1972 which used the Doppler principle to measure myocardial velocities from the posterior left ventricular (LV) wall [1]. Development in tissue Doppler imaging in the 1990s allowed for imaging the myocardial velocity and the analysis of the segments independently of each other [2, 3].

These improvements facilitated the use of tissue Doppler imaging in evaluation of LV diastolic function and in the measurement of strain and strain-rate of each myocardial segments. Due to the limitations posed by the angle dependence of the Doppler beam, techniques based on real time, 2D echocardiography such as speckle tracking imaging were then provided [4]. This technique has been improved and is used to calculate twist and torsion [5].

Definition of the Main Parameters of Myocardial Mechanics [6, 7]:

– **Displacement (d):** The distance that a cardiac structure or myocardial element (e.g., a speckle) moves between

two consecutive frames. Displacement is measured in centimeters.

- **Velocity (v):** Displacement per unit of time or speed of a cardiac structure or speckle. It is measured in centimeters per second.
- **Strain (ε):** The fractional change in the length of a myocardial segment. Strain is unitless, usually expressed as a percentage. It is reported as positive or negative values (which reflect lengthening or shortening, respectively). It can be measured in longitudinal, circumferential and radial directions.
- **Strain rate (SR):** Rate of change in strain. It is usually expressed as 1/s or s^{-1}.
- **Segmental strain:** Strain values which can be expressed for each myocardial segment
- **Global strain:** Average value for the strain in all myocardial segments.
- **Territorial strain:** Strain value for each of the theoretical vascular distribution areas.
- **Rotation:** Rotational displacement of myocardium around the long axis of LV. It is expressed in degrees.
- **LV twist angle:** The absolute apex-to-base difference in LV rotation; also expressed in degrees.
- **Torsion:** base-to-apex gradient in the rotation angle along the long axis of the left ventricle, expressed in degrees per centimeter

Doppler Tissue Imaging (DTI)

Doppler tissue imaging is a Doppler echocardiographic technique that directly measures myocardial velocities. The intensity of the signals generated by the myocardium is higher than that generated by blood. Blood velocity usually exceeds that of the myocardium. These differences allow separation of myocardial signals from those of blood flow, using a low-pass filter.

The typical velocity of myocardium ranges from 0 to 20 cm/s and Doppler gain setting must be increased to adequately visualize DT wave forms [8].

DTI includes both color tissue Doppler and spectral pulsed Doppler (Fig. 12.1).
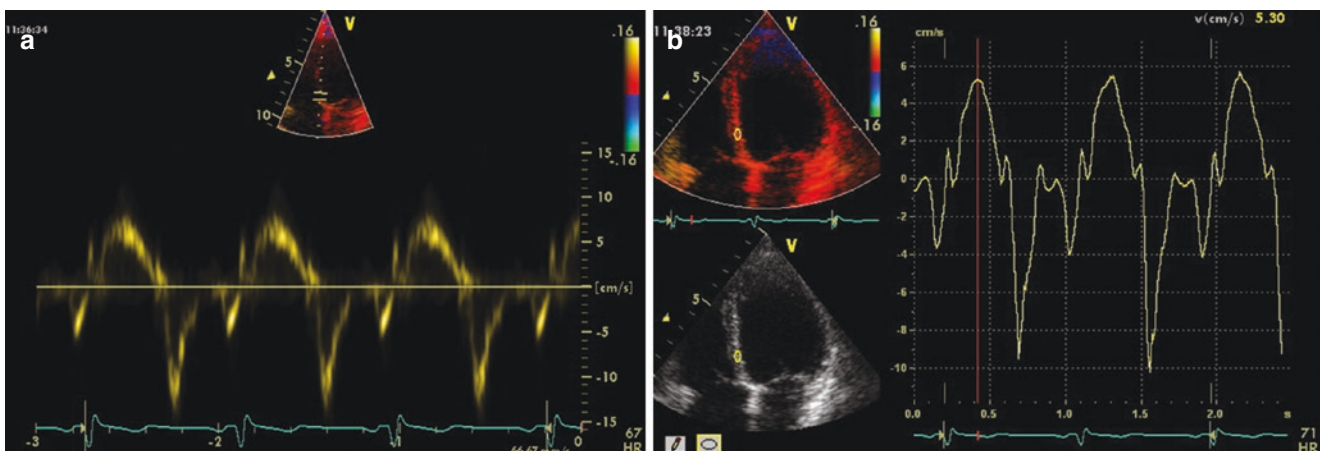
Spectral Pulsed Doppler

In this approach pulsed Doppler is activated and applied to measure mitral and tricuspid annulus velocities. Peak velocities, slopes, and time intervals are measured directly on the spectral display.

The Doppler velocities show systolic motion of the myocardium toward the apex which is the apical motion of the annulus in systole (Sm) (Fig. 12.2a). At diastolic phase, there is an early-diastolic motion away from the apex (Em), occurring at early phase of diastolic filling, and there is a late diastolic motion away from the apex, corresponding to the atrial phase of ventricular filing (Am).

Time intervals (ejection, isovolumic relaxation and isovolumic contraction time) could also be measured (Fig. 12.2b).

Some points are important to keep in mind while using spectral Doppler. Both sample volume and gain could influence the signal amplitudes and corresponding image quality. A sample volume should be set as 4–5 mm and position so that it remains within the region of interest inside the myocardium throughout the cardiac cycle. Excessive gain should be avoided, as this causes spectral broadening and may cause overestimation of peak velocity (Fig. 12.3).

The ultrasound beam should be aligned with the direction of the interrogated myocardial wall. The angle of incidence should not exceed 15°. So, the probability of velocity underestimation would be less than 4% (Fig. 12.4).

Fig. 12.1 Normal myocardial velocity obtained by spectral pulsed (**a**) and color tissue (**b**) Doppler modes
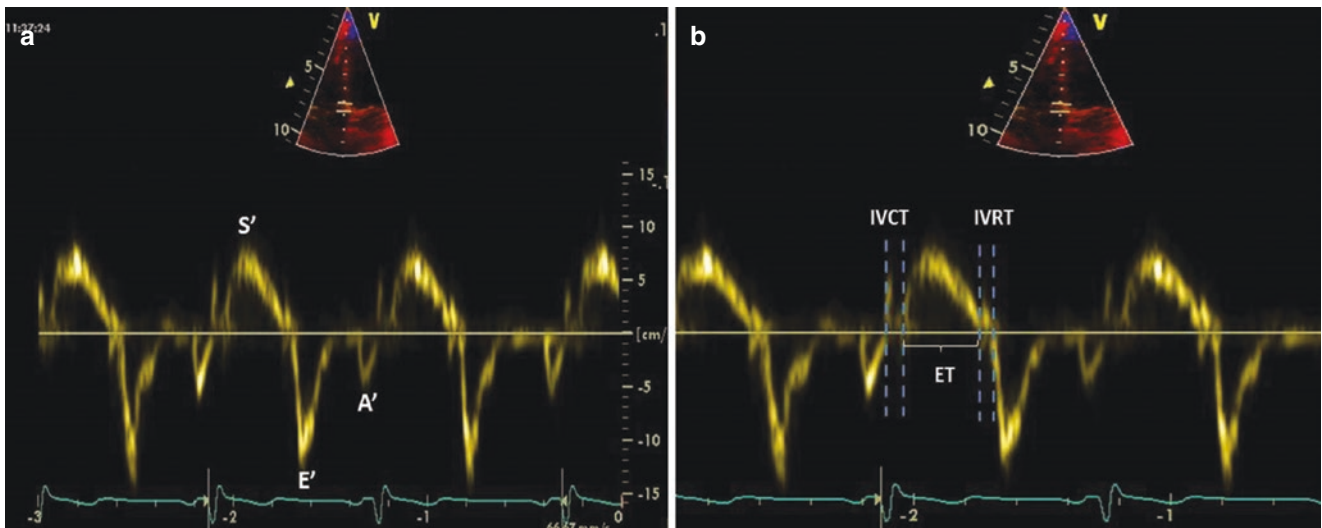
Fig. 12.2 Spectral Doppler obtained from septal side of mitral annulus, representing peak velocities (S′, E′ and A′) in A and time intervals (ET, IVCT and IVRT) in B
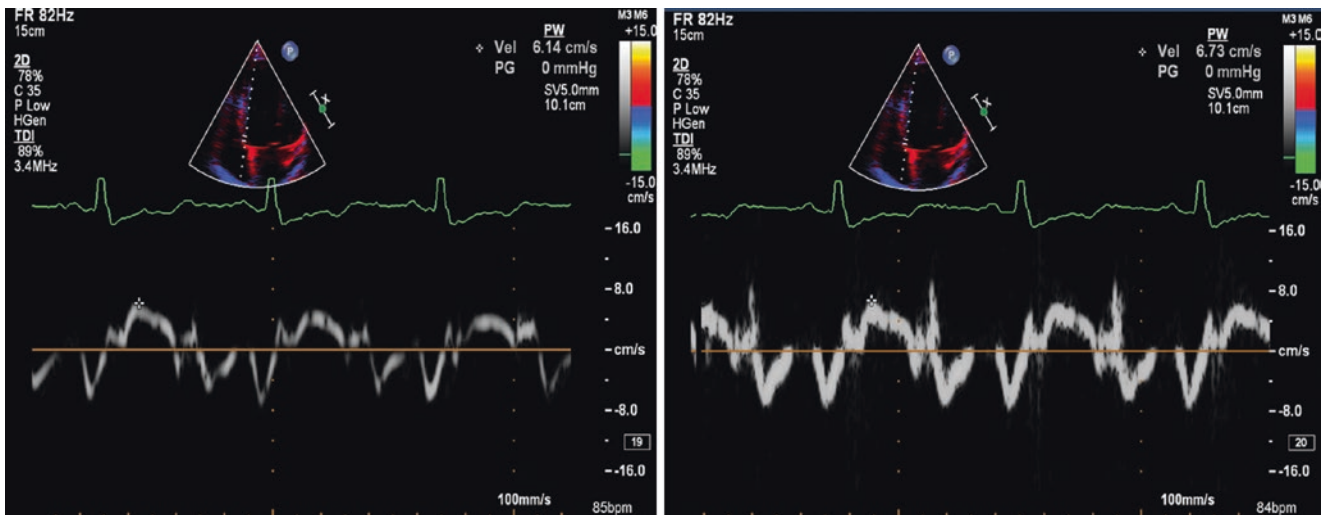
Fig. 12.3 Myocardial velocities by pulsed Doppler mode. The image in the right is obtained with a higher gain than for the left image. Consequently, the estimated S′ is higher (6.7 vs. 6.1 cm/s)

Color Tissue Doppler

In this approach, the myocardial motion is imaged as color-coded velocities superimposed on a 2D gray-scale image in real time (Fig. 12.5). At systolic phase, the base of ventricle moves toward the apex and in the diastole, moves back, while the apex is relatively stationery. These events are interrogated as red-encoded velocities in systolic phase and blue one in the diastole, in apical views.

The image should be optimized in the grayscale display before switching to the color mode and acquiring images [6]. Data can be displayed in three ways (Fig. 12.6):

1. Color coding with a straight M-mode.
2. Color coding with a curved M-mode.
3. Reconstructed curves of regional function.

This permits to track the changes in regional velocities and myocardial motion over the defined time course. Various function parameters can be derived from a selected region of interest (Fig. 12.7) within the same color Doppler data set, including velocity, displacement, SR, and strain.

To optimize the images, gain and depth adjustment, narrowing 2-D sector width (visualizing only the adjacent LV

Fig. 12.4 Alignment of the ultrasound beam with the myocardila wall is important, otherwise the measurement could be inaccurate and underestimated. Note the lower velocities in A vs. B in same patient
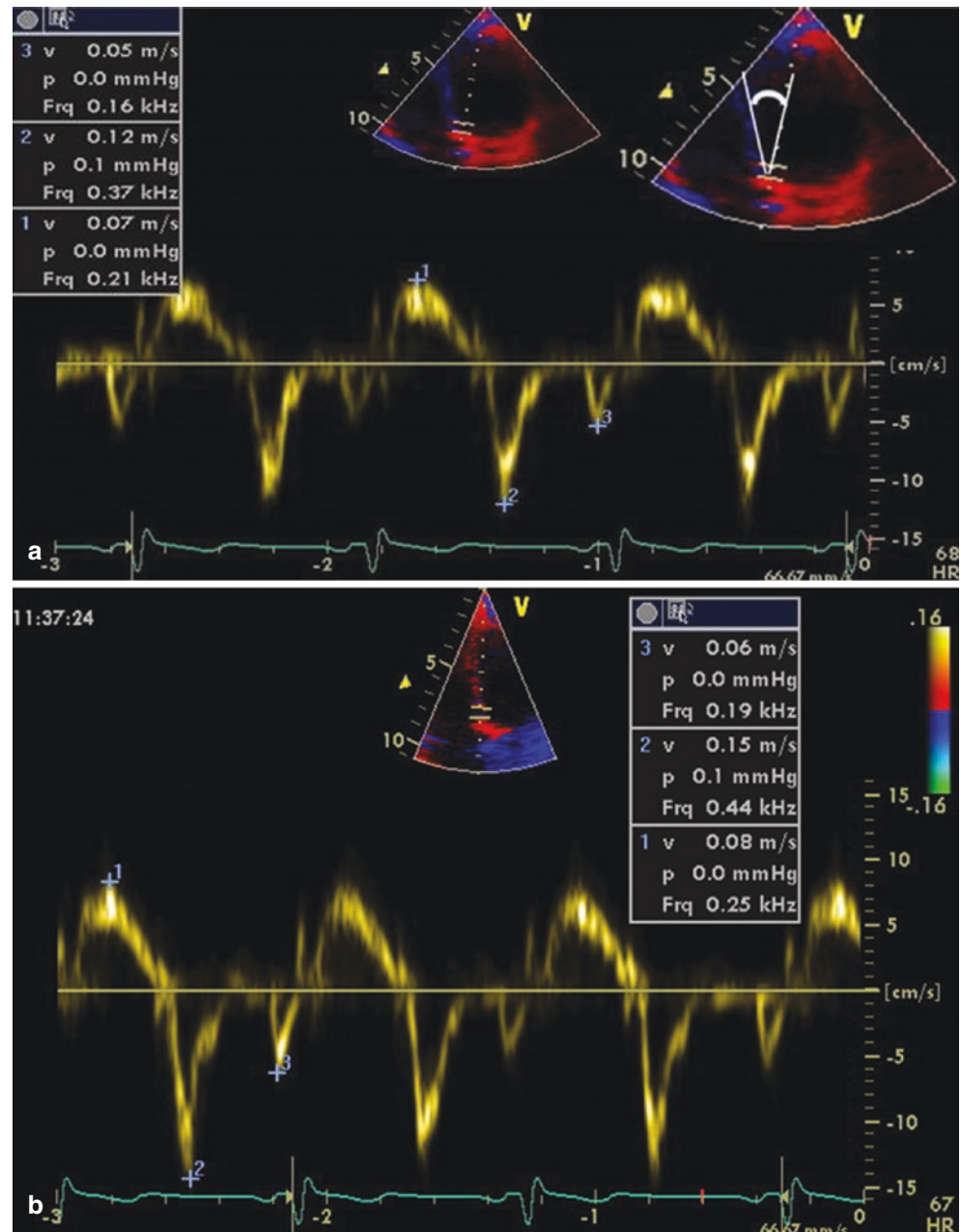

wall segments to be assessed) are necessary. Higher frame rate (as more than 100 and ideally at least 140) is suggested which could be achieved by reducing depth and sector width. The optimal sample size would be 10 mm × 5 mm. ROI placement should be positioned within the myocardium in such a way that doesn't move away the ventricular wall through the cardiac cycle.

Systolic and diastolic velocity curves (Sm, Em and Am) and the related time intervals could be reached, the same as spectral Doppler (Fig. 12.8).

There is a velocity gradient from the base to the apex with highest velocity at the base (Fig. 12.9).

Key Points
– The fundamental difference between Color Tissue and Spectral Pulsed Doppler is that the former provides the mean velocity in the region of interest, whereas PW Doppler provides the peak velocity at a given site. So that reported pulsed Doppler peak velocity is typically 20–30% higher than that measured by color Doppler.
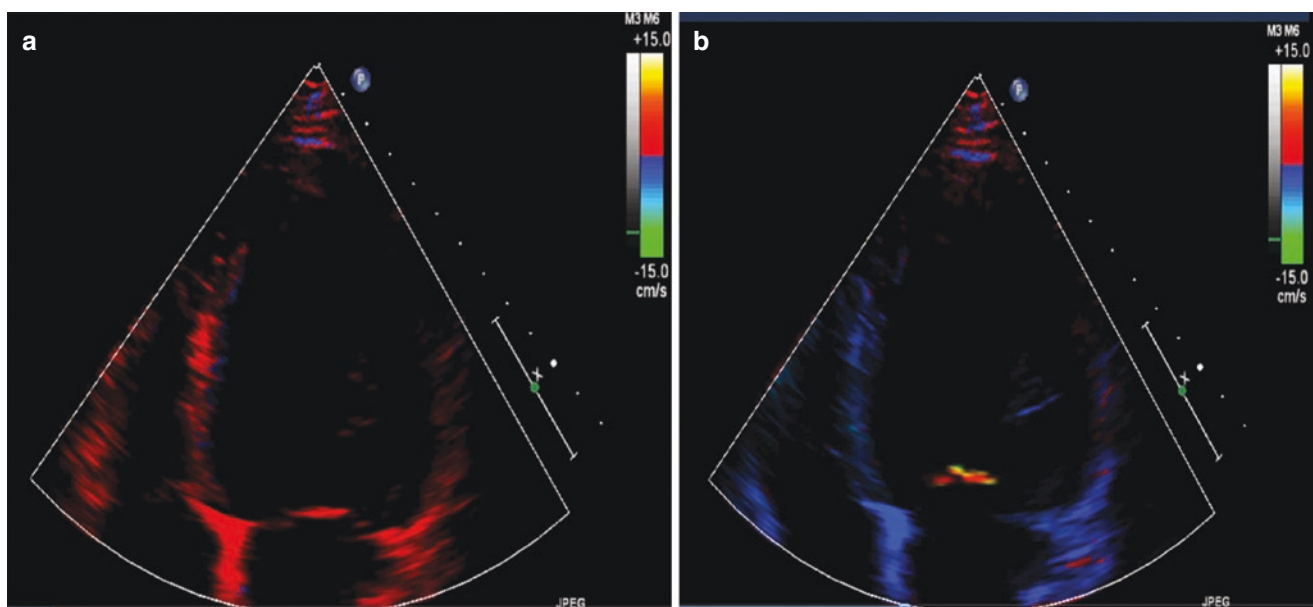
Fig. 12.5 Color coded TDI, in systole (**a**) vs. diastole (**b**); Note the red color in systolic phase in which the base of LV moves toward the apex (transducer) and blue color in diastole due to opposite motion
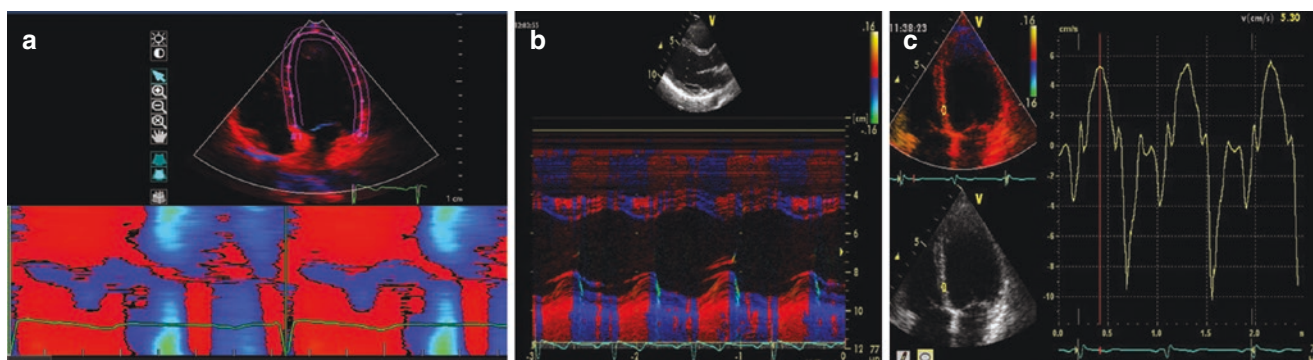
Fig. 12.6 Display of myocardial velocity in Color- coded DTI: (**a**) Curved M mode. (**b**) Straight M-Mode. (**c**) Reconstructed curves of regional function

– In Color Doppler, post processing is possible (adjusting the sample volume, not moving away the ventricular wall throughout a cardiac cycle and achieving multiple parameters of cardiac mechanics) and also we can sample different myocardial regions in the same time [6]. But in spectral Doppler, the data cannot be further processed.

Color Doppler Measurements of Cardiac Mechanics

Color DTI can provide displays of motion (velocity and displacement) and deformation (strain and strain rate)

(Fig. 12.10). The relation between these parameters is shown in Fig. 12.11.

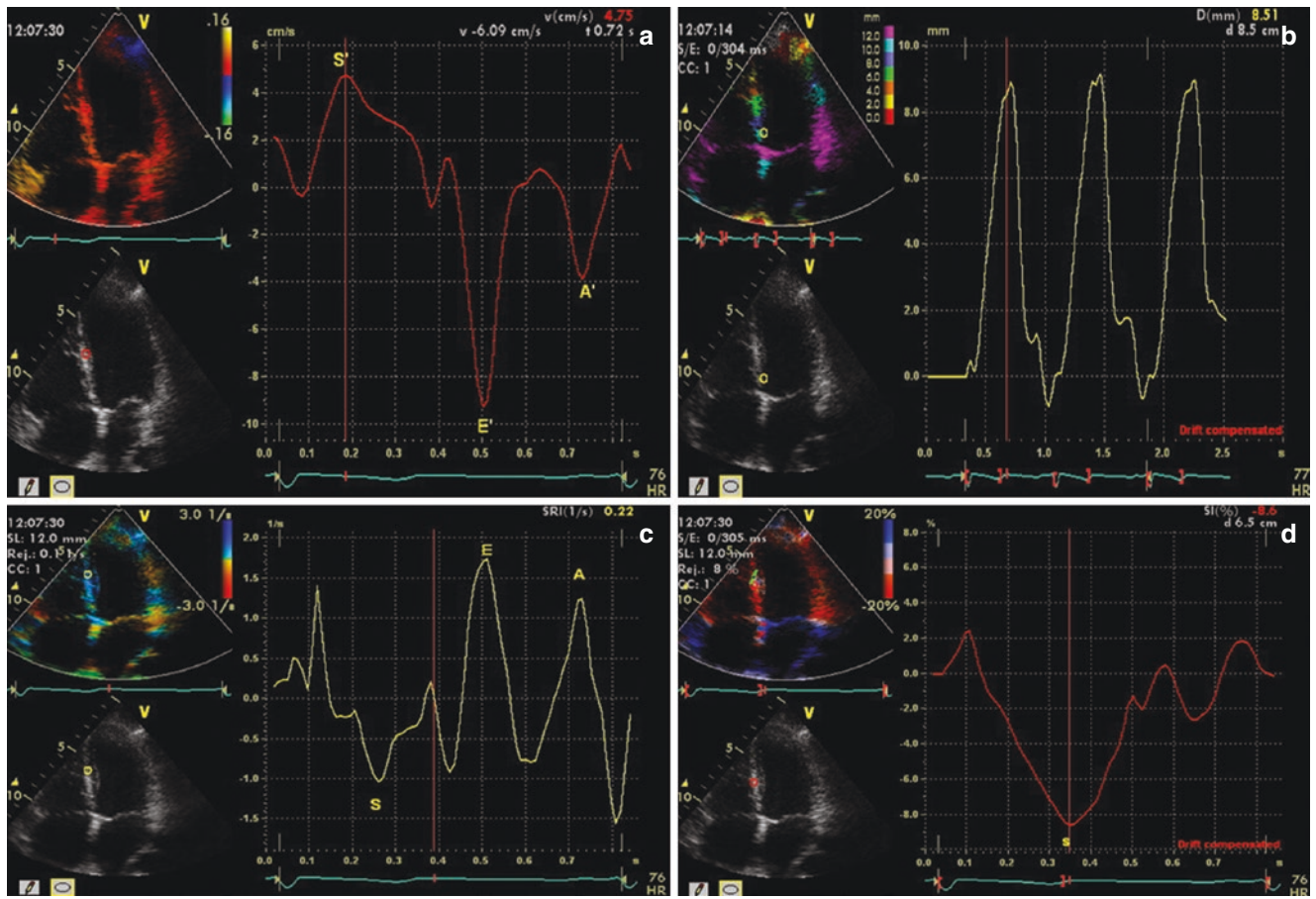The definition, formula and the way for obtaining the data of these four parameters are as follows:

1. Velocity (v):

   Doppler imaging provides velocity information. So, velocity at any site and any time can be achieved directly from the color Doppler data.
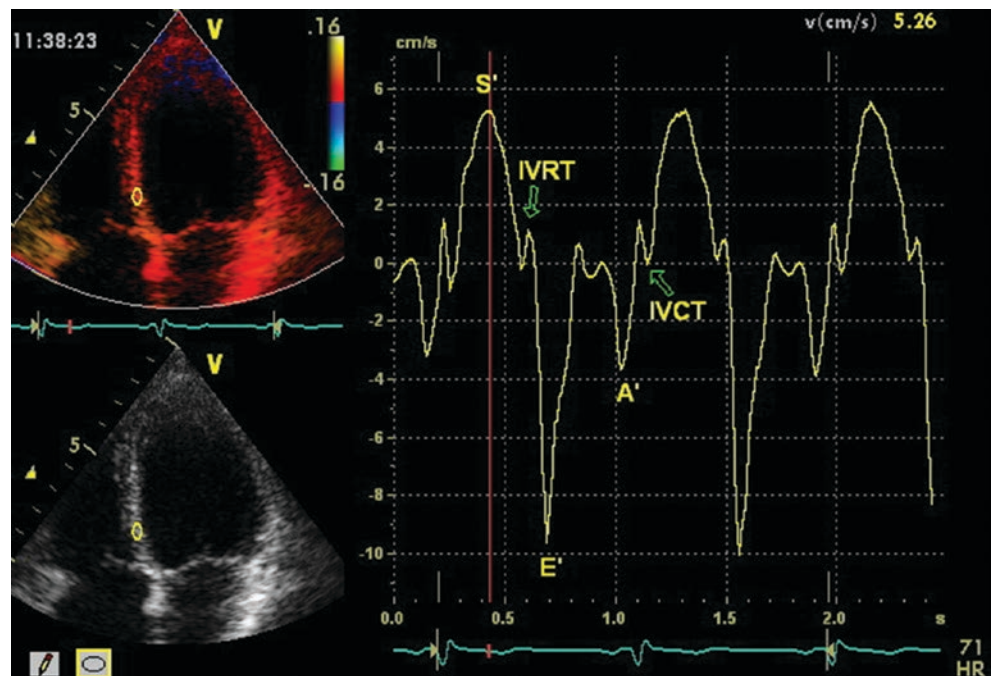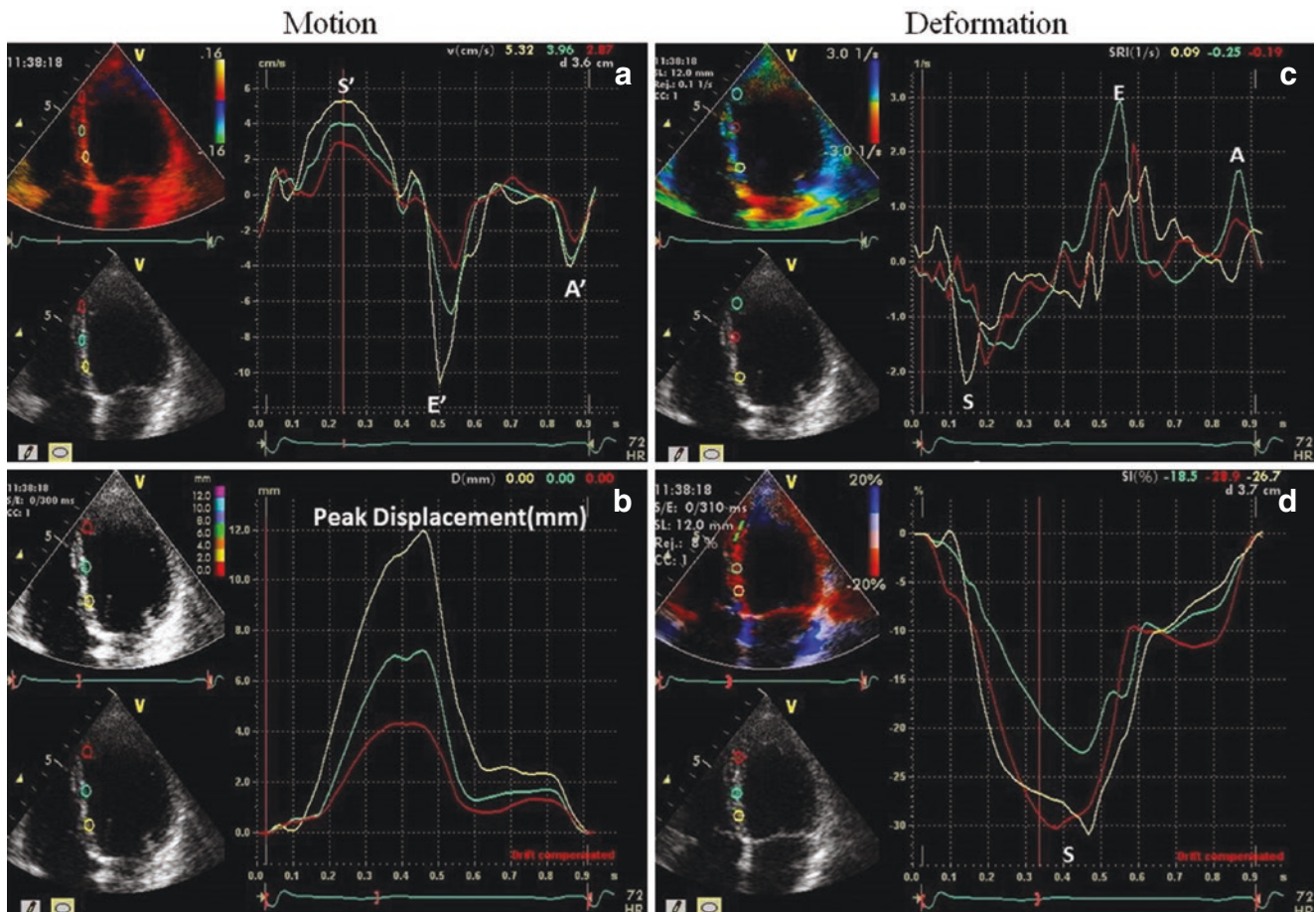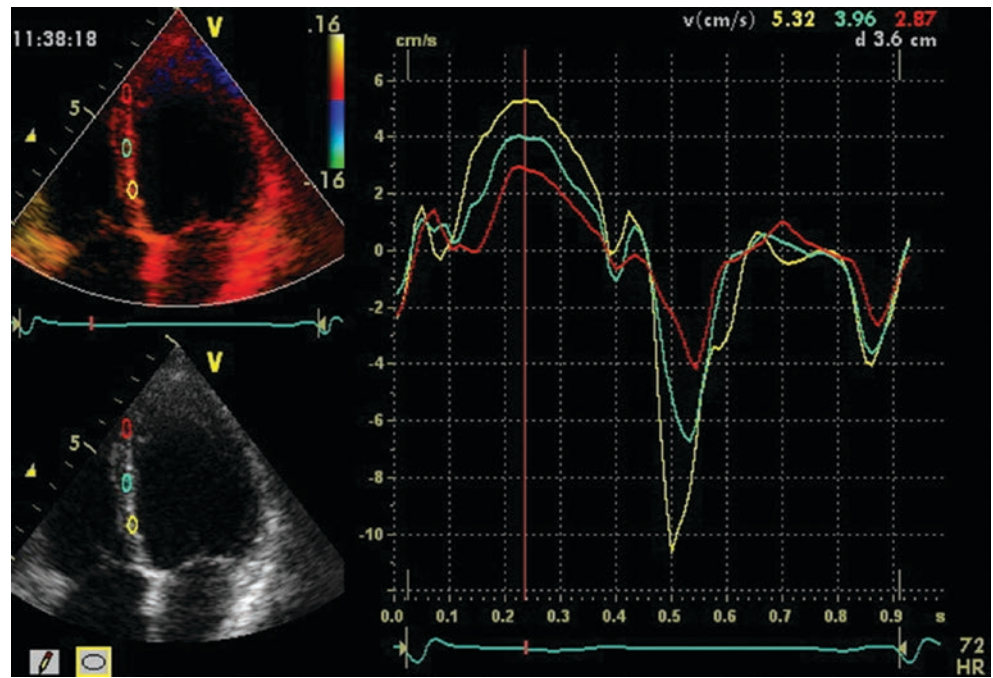
2. Displacement (d):

Fig. 12.7 Four parameter of myocardial function obtained from a single ROI in color coded imaging: (**a**) Myocardial velocity, (**b**) Displacement, (**c**) Strain Rate, (**d**) Strain

Fig. 12.8 Color Doppler wave form with ROI selected in septal segment of inferoseptum of LV; Peak velocities (S′, E′ and A′) and time intervals (IVRT, IVCT) could be derived

Fig. 12.9 Velocity curves obtained by color-coded DTI; Note the velocity gradient from the base to the apex

Fig. 12.10 Display of parameters of myocardial function defined as: (**a**) myocardial velocity, (**b**) Displacement, (**c**) Strain Rate, (**d**) Strain. Note the greater velocity and displacement in the base relative to the apex. Such gradient is relatively absent for deformation indices (strain/strain rate)

Displacement is obtained by calculating the temporal integral of the myocardial velocity (v):

$$d = \int v \, dt.$$

"d" describes the motion component of the myocardium in the sample volume (toward or away from the transducer).

Tissue tracking provides a color-coded display of myocardial displacement allowing for easy visualization of LV dyssynchrony and the region of latest activation.

3. Strain rate (SR) or rate of deformation (Fig. 12.12) equals the velocity gradient calculated as the difference of two instantaneous velocities (Velocity A and Velocity B) normalized for the distance (d) between the two velocity locations (A) and (B) as follows [6, 9]:

$$SR = \frac{Va - Vb}{d}$$

The strain rate signal displays compression in systole (expressed as negative value) and expansion (positive value)
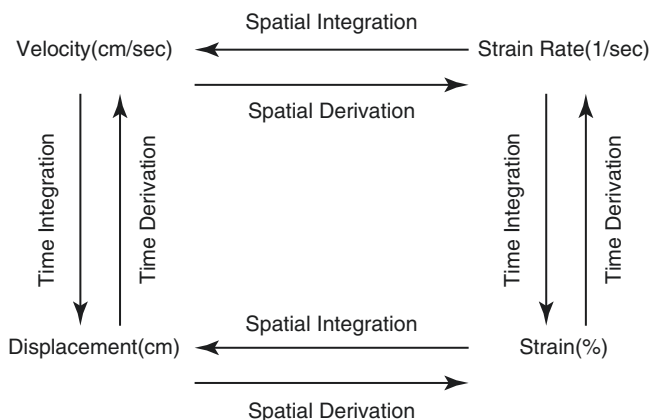
Fig. 12.11 The relation between four parameters of myocardial function

during diastole with three peaks that occur during isovolumetric relaxation and early and late diastole (Fig. 12.7c).

4. Strain (ε): Strain is a change in length between two locations from an initial length (L_0) to a new length (L).

Normalized to L_0 (Fig. 12.13). Thus strain can be expressed as: [10, 11]:

$$\varepsilon = (L - L_0) / L_0.$$

When deformation analysis is based on the initial length L_0, it is referred to as the Lagrangian strain, whereas when deformation is based on an previous time instance(and not original length), then so-called Eulerian (natural) strain is measured [12–14] such as by temporal integration of instantaneous strain rates in TDI (Fig. 12.11).

$$\varepsilon = \int SR \, dt$$

Natural strain is more relevant to cardiac imaging. At low strain (<10%), Lagrangian and natural strain can be used interchangeably [15].

For simplicity, in DTI, strain rate was derived from the gradient of velocity over a sampling distance, and strain obtained as the integral (Fig. 12.11).

Another method for measuring deformation indices is 2D–Speckle tracking echocardiography. In that technique, strain is derived from excursion of the speckles, and SR is derived from differentiation of the strain curve [15].

Key Points

Tissue Doppler velocities may be influenced by global heart motion (translation, torsion, and rotation), by movement of adjacent structures, and by blood flow. To minimize such effects, precise tracking of the myocardial segments and smaller sample size are suggested. However, the latter could result in noisier curves. The patient is asked to hold breathing for several heartbeats to reduce the effects of respiratory
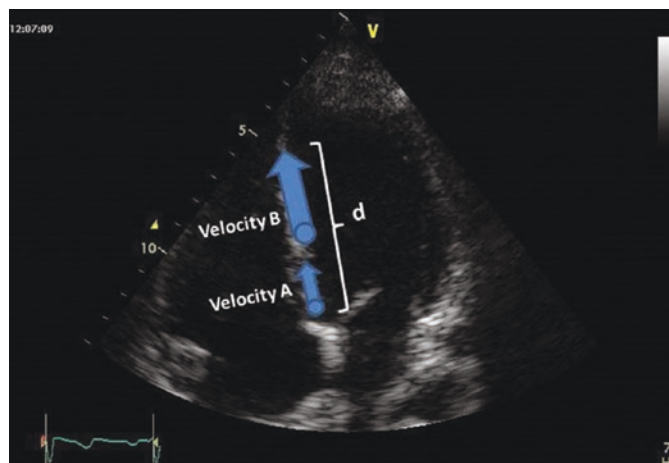
Fig. 12.12 Strain rate is the ratio between the difference in the velocities to the distance

$$SR = \frac{Vel\ A - Vel\ B}{d}$$

$$SR = \frac{\Delta\ Vel}{d} = 1/s$$

$$SR = \frac{\Delta\ Strain}{\Delta\ Time}$$

variation. The width of the imaging beam should be adjusted as narrow as possible [6].

Advantages and Disadvantages of DTI

It is readily available and allows objective quantitative evaluation of regional myocardial function.

Data of peak myocardial velocities are reproducible, which is essential for serial evaluations. Also, spectral pulsed DTI has excellent temporal resolution. Online measurements of velocities and time intervals are possible, which is crucial in evaluation of myocardial ischemia and diastolic function.

The major weakness of DTI is its angle dependency. It only measures velocities along the ultrasound beam, while velocities perpendicular to the beam remain undetected. In addition, only one segment can be examined at a time.

Color Doppler-derived strain and SR are noisy. Its temporal resolution is not as good as spectral Doppler (due to its lower frame rate). Training and experience are needed for proper interpretation and detecting artifacts.

In principle, strain/strain rate is not influenced by overall motion of the heart (translation) or by motion caused by contraction in adjacent segments (in contrast to velocity within a myocardial segment that cannot distinguish active from passive deformation.)

Two-Dimensional Speckle-Tracking Echocardiography (2D–STE)

STE is a relatively new, largely angle-independent method for the evaluation of myocardial function. The speckles seen in gray scale images are the result of interference of ultrasound backscattered from structures smaller than the ultrasound wavelength (Fig. 12.14).

Blocks or kernels of speckles can be tracked from frame to frame (simultaneously in multiple regions within an image plane) using block matching, and provide local displacement

End Systolic Phase   End Diastolic Phase
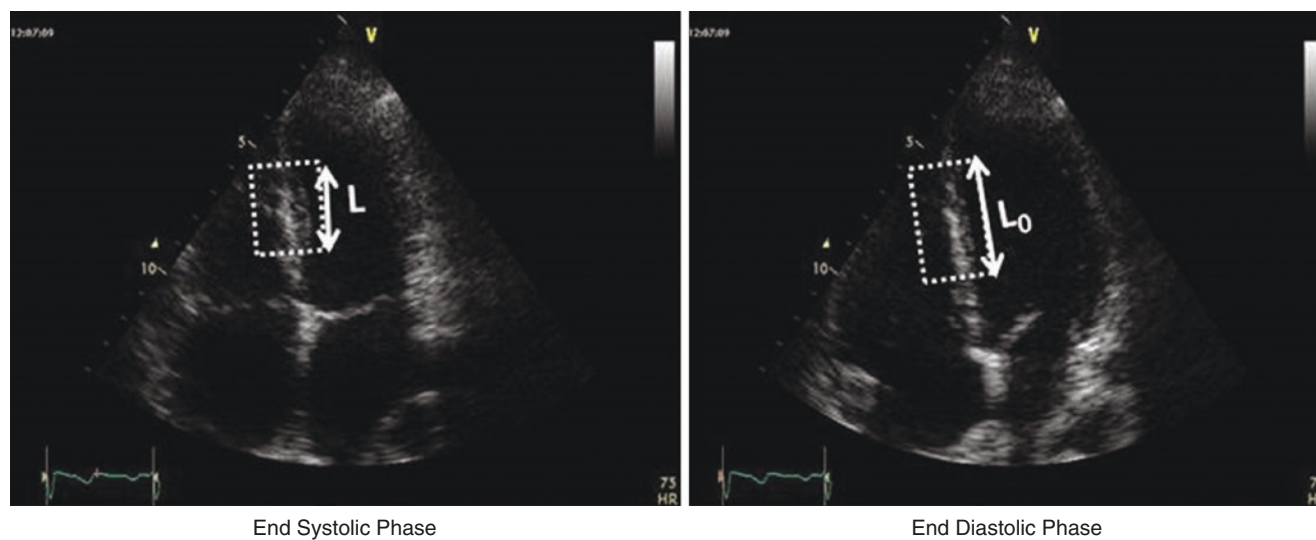
Fig. 12.13 Strain is calculated by the changes in length normalized to the initial length
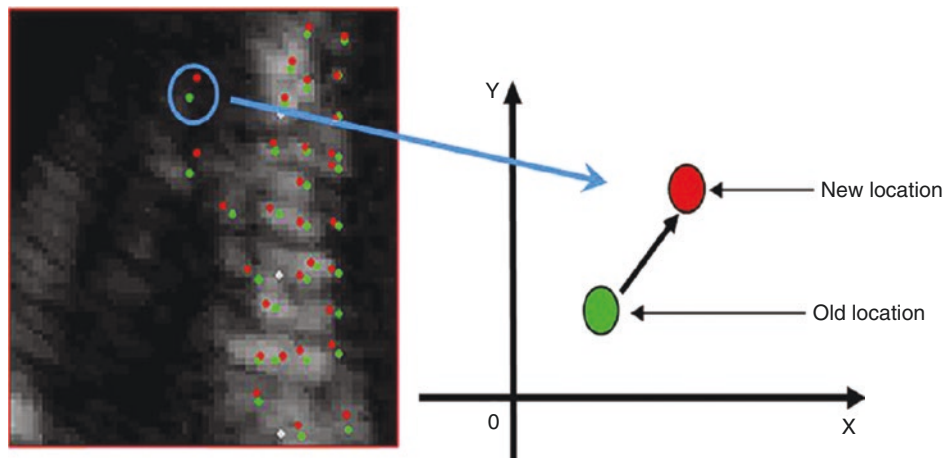
Fig. 12.14 The principle of STE. Myocardial speckles in a gray-scale image are tracked frame-by-frame. So, the myocardial deformation in different directions could be achieved [53, 54]

information, from which parameters of myocardial function such as velocity, strain, and SR can be derived [6].

quality of speckle tracking, and thus care should be taken to avoid these.

How to Optimize the Images in 2D–STE?

Frame rates of 40–80 frames/s is used in normal sinus rhythm [16] but higher frame rates are advisable to avoid undersampling in tachycardia [17]. The focus is placed at an intermediate depth, and sector depth and width should be adjusted to include as little as possible outside the region of interest. Any artifact that resembles speckle patterns will influence the

Types of Strain

LV contraction involves myocardial motion along three-dimensional (3D; x, y, and z) coordinates and results in a variety of strain parameters that can be derived for each myocardial segments.

Consequently, different type of strain could be achieved [18] (Fig. 12.15):
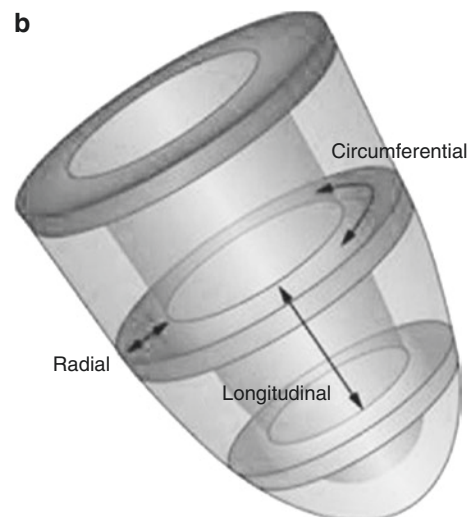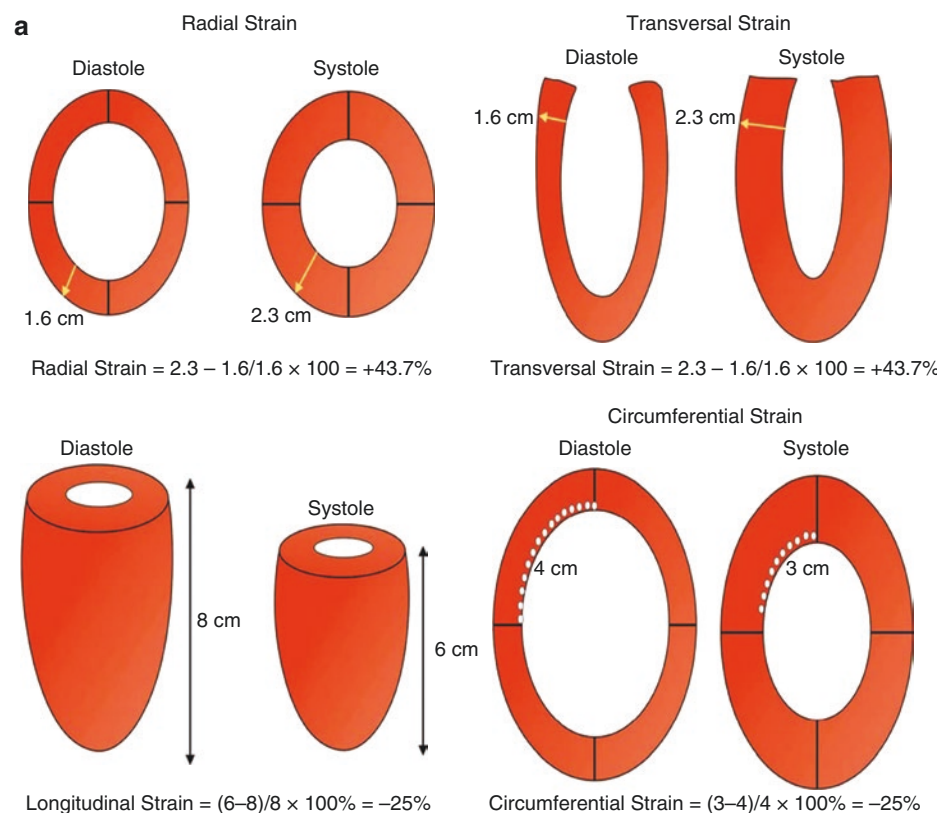
**Fig. 12.15** (**a**, **b**) Schematic views of different types of strain: Radial strain; transverse strain (similar to radial strain, except that the measurements are done using apical views. Longitudinal strain. Circumferential strain. Radial and circumferential strain are derived from short axis views in contrast to longitudinal and transverse strain which are achieved from apical, long axis views [33]

1. Longitudinal strain: Changes in the longitudinal length of myocardium (negative value during systole).
2. Radial Strain: changes in myocardial thickness in short axis, e.g., myocardial thickening with inward motion of LV in systole presenting as positive value at this phase.
3. Transverse Strain: Changes in myocardial thickness in apical view, e.g., myocardial thickening with inward motion of LV in the systole, presenting as positive value.
4. Circumferential Strain: Changes in the length measured circumferentially around the perimeter of LV (presented as negative value in the systole).
5. Rotational Strain: Rotational myocardial motion along the long axis of LV (with clockwise rotation represented as negative value and vice versa.)
6. Twist and untwist: Difference in rotation between apex and base. Twist is used for systole and untwist for the diastolic phase.

Other type of strain not routinely used in echocardiography is shear strain [11].

The timing at which peak strain is measured is not uniform across publications. Peak strain can be measured as peak systolic strain (positive or negative), peak strain at end-systole (at time of aortic valve closure, AVC), or peak strain regardless of timing (in systole or early diastole).

End systolic strain, may be exceeded by peak strain, and the difference normalized to the peak strain is usually measured as post systolic index (PSI) (Fig. 12.16).
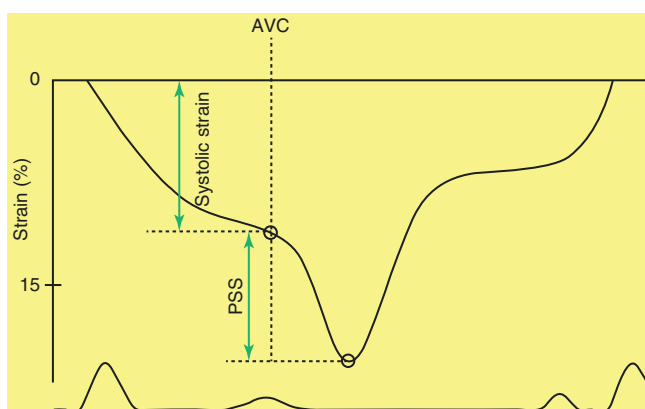
Fig. 12.16 PSS is higher than end systolic strain (measured at aortic valve closure) in this image. Difference in the magnitude of strain and also the time interval have been used in myocardial ischemia (Reduced systolic strain, PSS exceeding 20% of total strain or occurring more than 90 milliseconds after AVC signify pathologic state). *AVC* Aortic valve closure; *PSS* postsystolic shortening. Adapted from Voigt et al. Incidence and characteristics of segmental postsystolic longitudinal shortening in normal, acutely ischemic, and scarred myocardium. J Am Soc Echocardiogr. 2003

Global Strain

Segmental strain is calculated in the three apical views (segmental strain in the apical four- and two-chamber and long axis views) and then averaged as GLS, combined in a polar map (Figs. 12.17, 12.18, 12.19, 12.20, 12.21, 12.22, 12.23, and 12.24).

2D-STE Analysis of Myocardial Mechanics

Two-dimensional STE allows measurements of the above four parameters of myocardial mechanics by tracking groups of intramyocardial speckles (d or v) or myocardial deformation (ε or SR) in the imaging plane. When automated tracking does not fit with the visual impression of wall motion, regions of interest need to be adjusted manually until optimal tracking is achieved.

For the left ventricle, because end-systole can be defined by aortic valve closure as seen in the apical long-axis view, this view should be analyzed first.

Assessment of 2D strain by STE can be applied to both ventricles and atria. However, because of the thin wall of the atria and right ventricle, signal quality may be suboptimal. In contrast, all LV segments can be analyzed successfully in most patients. Feasibility is best for longitudinal and circumferential strain and is more challenging for radial strain.

Pitfalls of 2D STE

1. Suboptimal tracking of the endocardial border.
2. Sensitivity to acoustic shadowing or reverberations.

Both of them could result in under -estimation of the true deformation or non-physiologic traces [19].

Advantages and Disadvantages of 2D- STE

Although both DTI and STE measure myocardial motion against a fixed external point in space (i.e., the transducer), STE is able to measure this motion in any direction within the image plane. In contrast, DTI is just capable to define the velocity component toward or away from the probe. So, STE could measure circumferential and radial components irrespective of the direction of the beam (Table 12.1).

– STE is not completely angle independent. It works better for measuring deformation along the ultrasound beam than in other directions.
– STE relies on good image quality. The details can be tracked from one frame to the next and when out of plane motion does not occur.
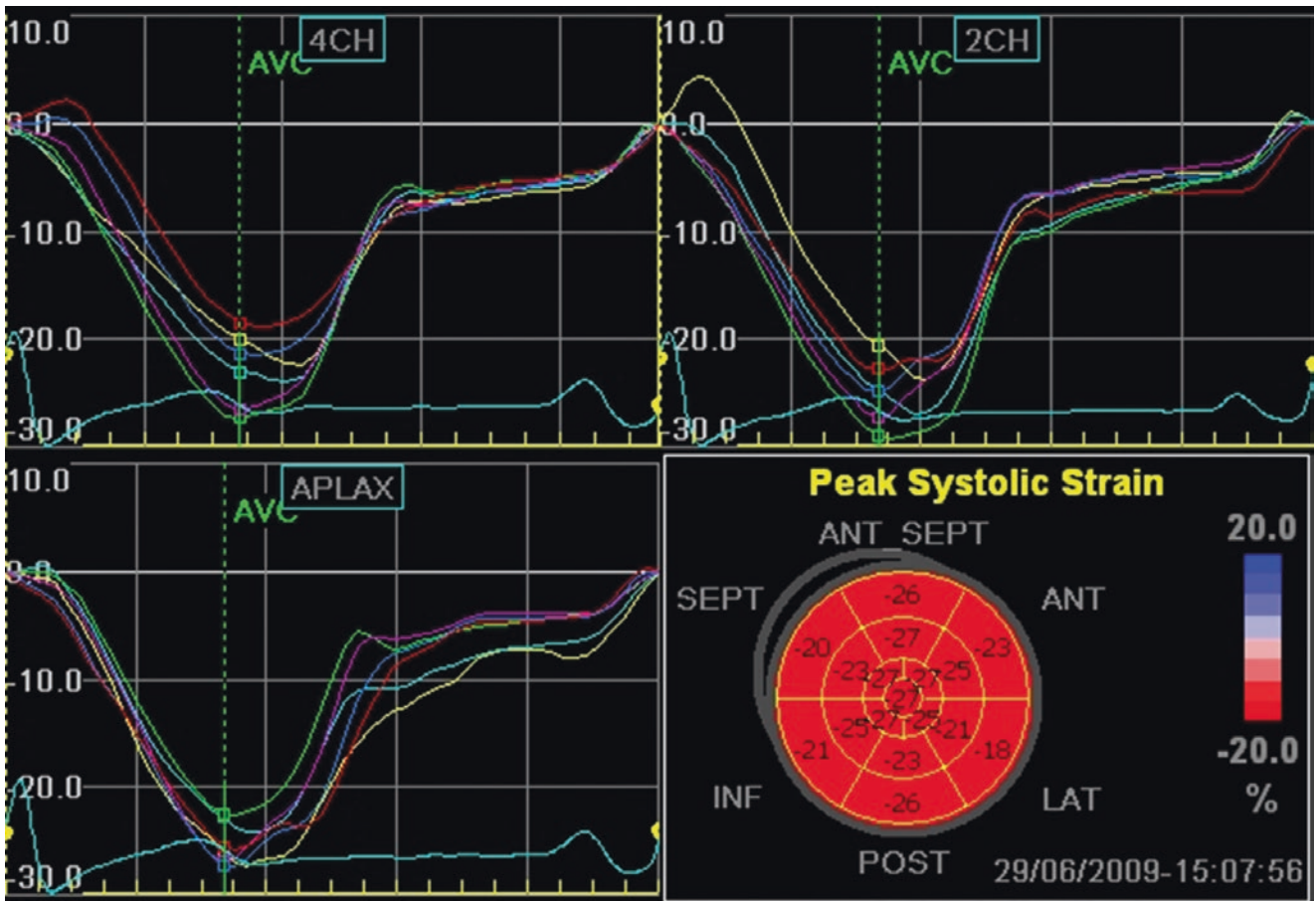
Fig. 12.17 Segmental longitudinal systolic strain curves derived from three apical views

Fig. 12.18 Normal 17-segments Bull's eye template showing myocardial longitudinal strain in each myocardial region. Global longitudinal strain was presented as −24.1% in this case

Fig. 12.19 17-segments Bull's eye template showing myocardial longitudinal strain in a case with infero-posterior MI and reduced strain in related segments. Global longitudinal strain was presented as −16.1% in this case

Fig. 12.20 17-segments Bull's eye template showing myocardial longitudinal strain in a case with end stage Dilated Cardiomyopathy and severely reduced strain in all segments. Global longitudinal strain was presented as −6.3% in this case
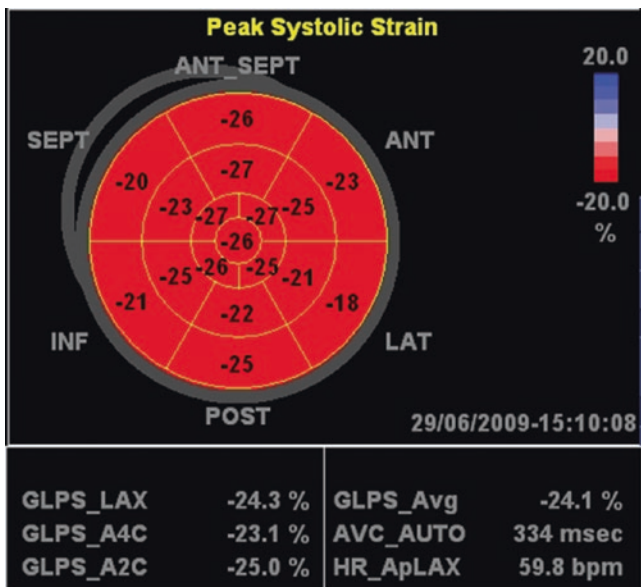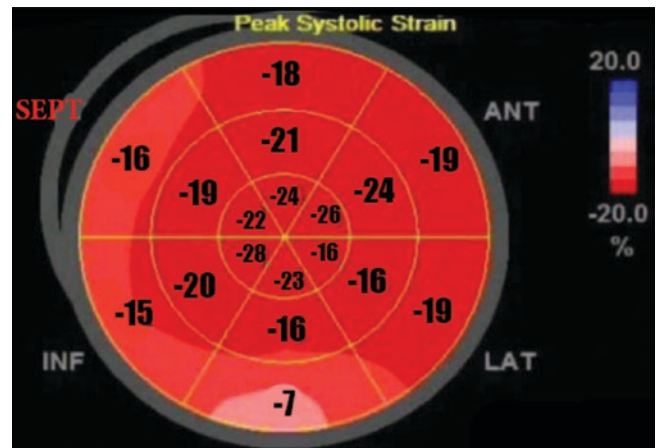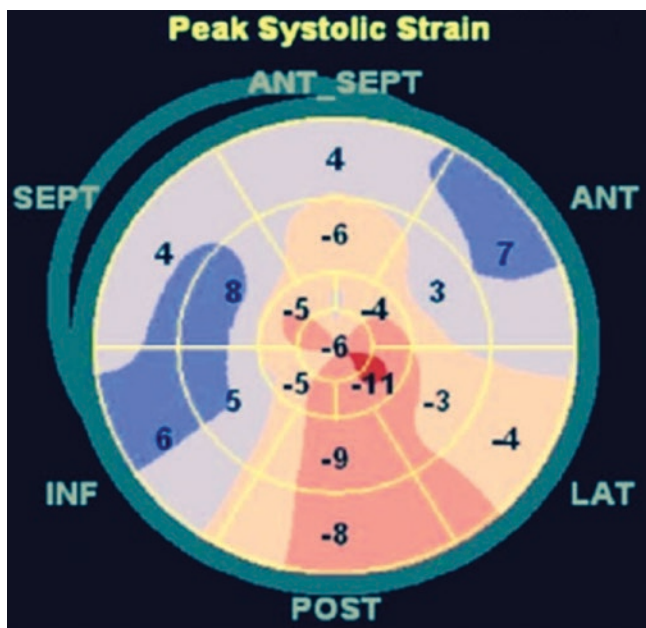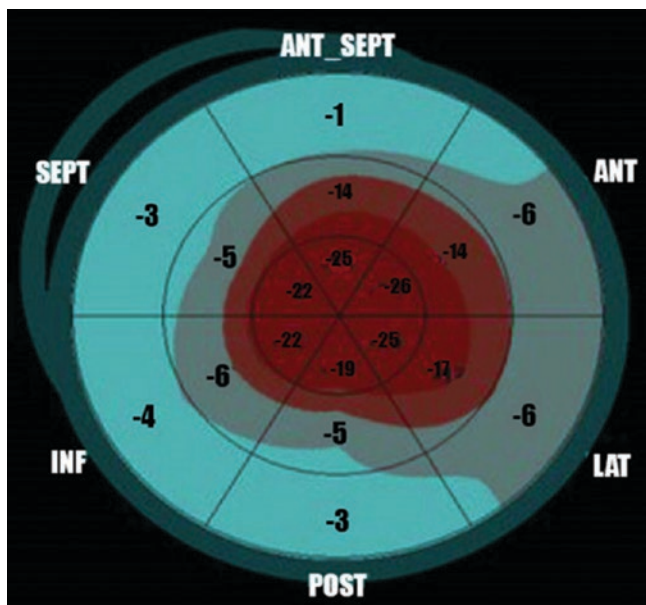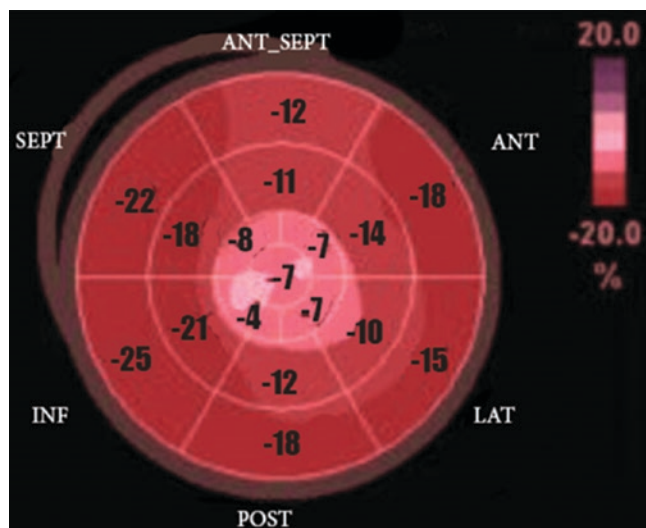

Fig. 12.21 17-segments Bull's eye template showing myocardial longitudinal strain in a case with Hypertrophic Cardiomyopathy and reduced strain in basal and mid hypertrophied segments. Global longitudinal strain was presented as −10.1% in this case

Fig. 12.22 17-segments Bull's eye template showing myocardial longitudinal strain in a case with apical Hypertrophic Cardiomyopathy and reduced strain in apical hypertrophied segments. Global longitudinal strain was presented as −16.8% in this case

Fig. 12.23 17-segments Bull's eye template showing myocardial longitudinal strain in a case with Restrictive Cardiomyopathy and reduced strain in basal segments and preserved red color apical segments. Global longitudinal strain was presented as −7.8% in this case

– In higher rate or while measuring short living time intervals (e.g., IVRT), DTI prove to be more useful (due to its higher temporal resolution).
– A significant limitation of the current implementation of 2D STE is the differences among vendors.

Three-Dimensional STE

The entire left ventricle can be analyzed from a single volume of data obtained from the apical transducer position. So, its use was found to considerably reduce the examination time to one third of that for 2D STE [6]. In contrast to 2D
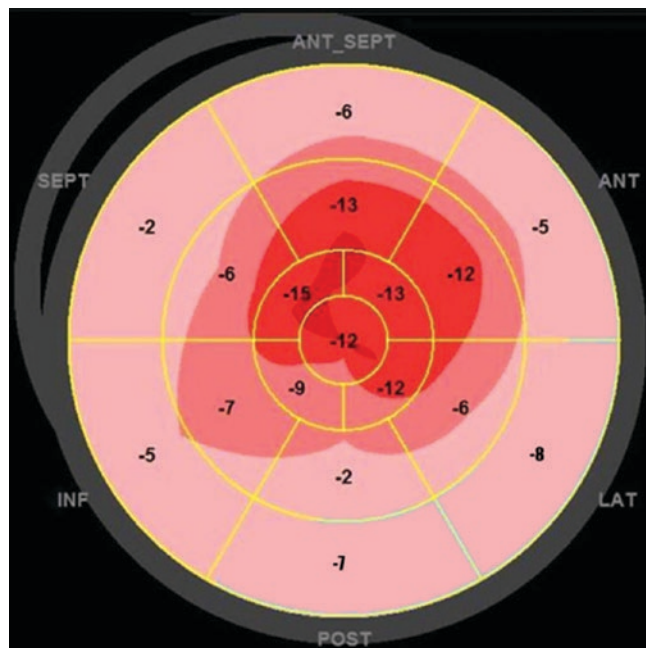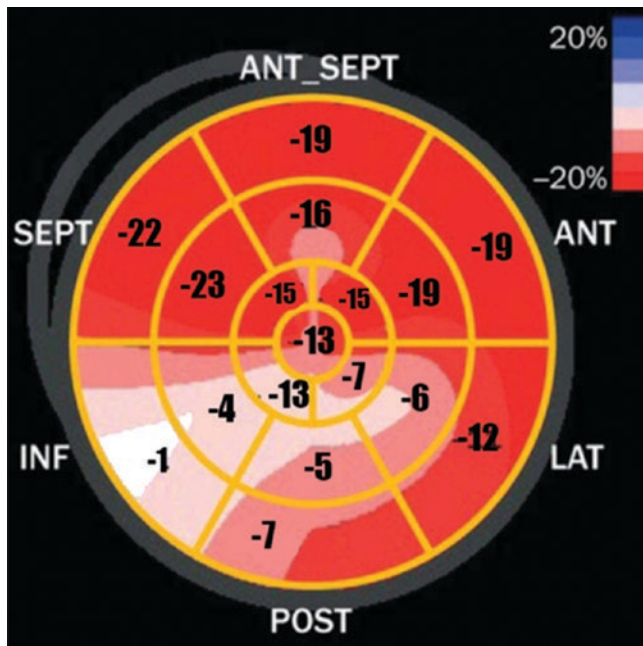
Fig. 12.24 17-segments Bull's eye template showing myocardial longitudinal strain in a case with Constrictive Pericarditis and reduced strain in inferior, posterior and lateral segments. Global longitudinal strain was presented as −14% in this case

Table 12.1 Comparison between DTI with 2D–STE for evaluation of strain

Tissue Doppler imaging	Speckle tracking
Dependent on the angle between ultrasound angle and the interrogated wall	Relatively angle independent
Strain is derived from tissue velocity	Strain and strain rate could be measured directly
Deformation could be measured along the axis of insonation	Longitudinal, radial and circumferential strain and also LV twist could be measured
Movement assessed in relation to the transducer	Movement assessed in relation to the adjacent speckles
Limited Spatial resolution but higher frame rate and temporal resolution	Better spatial resolution but poor temporal resolution (limited utility in tachycardia or non-sinus rhythm)
Assess only regional strain	Assess both regional and global strain
Influenced by translational motion	Less influenced by translational motion
Less reproducibility	Less inter- and intra -observer variability

Modified table from Biswas M et al. Two- and three-dimensional speckle tracking echocardiography: clinical applications and future directions. Echocardiography. 2013;30(53):88–105

STE, which cannot track motion in and out of the imaging plane and measure only one of the three components of the local displacement vector, the recently developed 3D STE can track motion of speckles irrespective of their direction, as long as they remain within the selected scan volume.

3D STE based measurements of LV volumes were found to be in close agreement with magnetic resonance-derived refer-

ence values. The agreement were higher than those of 2D STE measurements [20, 21]. It can be applied using full volume mode, including the entire LV cavity within the pyramidal volume. This could obviously reduce the temporal resolution.

Advantages and Disadvantages

Assessment of regional myocardial dynamics could be accurate due to addition of the third component of motion vector. Nevertheless, it still requires more validation. It has much slower frame rates of 3DE compared with 2D STE. So, the analysis of rapid events such as isovolumic contraction and relaxation would be inaccurate. In addition, it is dependent on image quality, has random noise, lower spatial and as noted temporal resolution. These limitations could result in sub-optimal myocardial tracking.

Normal Values of LV Myocardial Mechanics

The normal values vary depending on the specific LV wall and the specific 3D component of each index. Longitudinal velocities in the lateral wall are higher than in the septum. There is also a base-to-apex gradient (with higher velocities recorded at LV base than near the apex).

Minor differences are seen between LV segments for DTI-derived strain and SRs.

STE-derived measurements generally show higher values in the apical segments than DTI. Within a segment, higher velocities and strains are usually recorded from the sub-endocardium than from the sub-epicardium. Velocities and deformation parameters are also affected by age (Table 12.2) and loading conditions.

The lower limits of normal range with the Doppler method were found to be –18.5 and 44.5% for longitudinal and radial strain and –1.00 and 2.45 s^{-1} for longitudinal and radial SR [22].

Normal range for different types of strain in normal adults are shown in Table 12.3.

In Table 12.4, the normal range of strain rate (in three phase of cardiac cycle: S, E and A) and displacement have been provided.

Normal values for GLS also depend on the vendor, resulting in considerable heterogeneity in the published literature (Table 12.5).

To provide some guidance, a peak GLS in the range of –20% can be expected in a healthy person [6, 23].

Clinical Use of LV Displacement, Velocity, Strain, and SR

The following is a brief summary of parameters of myocardial function in multiple disease states, gathered as Table 12.6.

Table 12.2 Normal Values for mitral andtricuspid annulus velocity by TDI in healthy volunteer

	LV (mean of four walls)				RV (free wall)		
	S'(pwTDI)	S'(cTDI)	E'(pwTDI)	A'(pwTDI)	S'(pwTDI)	E'(pwTDI)	A'(pwTDI)
Female	8.2 ± 1.3	6.6 ± 1.1	11.8 ± 3.2	9.7 ± 2	12.5 ± 1.9	13.3 ± 3.0	14.4 ± 3.7
Male	8.6 ± 1.4	6.9 ± 1.3	10.8 ± 3.0	10.3 ± 1.7	12.8 ± 3.3	12.5 ± 3.3	14.2 ± 3.9

Modified table from Dalen H, Thorstensen A, Vatten LJ, et al.: Reference values and distribution of conventional echocardiographic Doppler measures and longitudinal tissue Doppler velocities in a population free from cardiovascular disease. *Circ Cardiovasc Imaging* 3(5):614–622, 2010

Table 12.3 Normal values of different type of strain, considering the interrogated wall or segment

	Interrogated segment	Apicoseptal	Mid septal	Basal septal	Apical lateral	Mid lateral	Basal lateral
Longitudinal strain	Value	–21 ± 4	–19 ± 4	–17 ± 4	–21 ± 7	–19 ± 6	–19 ± 6
Circumferential strain	Interrogated wall	Anterior	Lateral	Posterior	Inferior	Septal	Anteroseptal
	Value	–24 ± 6	–22 ± 7	–21 ± 7	–22 ± 6	–24 ± 6	–26 ± 11
Radial strain	Interrogated segment	Anterior	Lateral	Posterior	Inferior	Septal	Anteroseptal
	Value	39 ± 16	37 ± 8	37 ± 17	37 ± 17	37 ± 19	39 ± 15

Modified table from: Hurlburt HM, Aurigemma GP, Hill JC. Direct ultrasound measurement of longitudinal, circumferential, and radial strain using two-dimensional strain imaging in normal adults. Echocardiography. 2007; 24:723–31

Table 12.4 Normal ranges of SR and displacement have been defined at each phase of the cardiac cycle in four LV walls

	Septum	Lateral	Inferior	Anterior
Peak systolic wave (Ssr)				
Basal	–0.99 ± 0.49	–1.5 ± 0.74	–0.88 ± 0.39	–1.64 ± 0.9
Mid	–1.25 ± 0.73	–1.29 ± 0.58	–0.95 ± 0.54	–0.98 ± 0.68
Apical	–1.15 ± 0.5	–1.09 ± 0.59	–1.38 ± 0.45	–1.05 ± 0.63
Early diastolic wave (Esr)				
Basal	1.95 ± 0.89	1.92 ± 1.11	1.85 ± 0.89	2.03 ± 0.99
Mid	1.94 ± 0.97	1.71 ± 0.66	1.92 ± 1.2	1.7 ± 0.82
Apical	1.91 ± 0.66	1.81 ± 0.87	2.29 ± 0.88	1.76 ± 0.98
Late diastolic wave (Asr)				
Basal	1.54 ± 0.93	0.93 ± 0.59	1.18 ± 0.78	1.49 ± 0.96
Mid	1.29 ± 0.86	1.48 ± 0.77	0.78 ± 0.62	1.04 ± 0.57
Apical	0.95 ± 0.54	1.07 ± 0.68	1.68 ± 0.76	0.68 ± 0.65
Displacement (D)				
Basal	1.2 ± 0.19	0.93 ± 0.22	1.33 ± 0.22	1.05 ± 0.27
Mid	1.13 ± 0.27	0.91 ± 0.18	0.62 ± 0.22	1.04 ± 0.19
Apical	0.65 ± 0.24	0.82 ± 0.27	0.55 ± 0.18	0.41 ± 0.25

Modified table from: Gillam LD, Otto CM. Advanced Approaches in Echocardiography. Philadelphia, PA: Elsevier Saunders; 2012, p 85 (Table 6.1)

Twist, Rotation and Torsion

Rotation describes the wringing motion of the heart from contraction of its obliquely oriented muscle bundles. This deformation can be quantified by both tissue Doppler imaging and speckle tracking. Adequate short axis images of the LV apex and base are essential for this measurement. From the view of the apex, the apex rotates counterclockwise in systole (during ejection) and the base rotates clockwise [31].

Table 12.5 Normal LV strain using specific vendors

Vendor	Software	Mean ± SD	LLN (%)
GE	EchoPAC BT 12	−21.5 ± 2.0%	−18
		−21.5 ± 2.0%	−18
		−21.2 ± 2.4%	−17
	EchoPAC 110.1.3	−21.3 ± 2.1%	−17
Philips	QLAB 7.1	−18.9 ± 2.5	−14
Toshiba	Ultra Extend	−19.9 ± 2.4%	−15
Siemens	WI	−19.8 ± 4.6	−11
	WI	−17.3 ± 2.3	−13
Esoate	Mylab 50	−19.5 ± 3.1	−13

LLN lower limit of normal

Modified table from: Lang RM, Badano LP, Mor-Avi V, Afilalo J, Armstrong A, Ernande L, et al. Recommendations for Cardiac Chamber Quantification by Echocardiography in Adults: An Update from the American Society of echocardiography and the European Association of Cardiovascular Imaging. J Am Soc Echocardiogr. 2015;28:1–39

In late systole and early diastole (the isovolumetric relaxation period and briefly during early LV filling), the apex and base reverse-rotate at the same speed and to the same degree as in systole [32].

By convention, clockwise rotations carry a negative value and counterclockwise rotations are assigned a positive value.

LV systolic twist is defined as the difference between the apical and basal rotations.

$$\text{Twist} = \text{Apex} - (\text{Base}),$$

In normal controls [33], apical rotation is 6° and basal rotation is –6°, producing a twist of 12°.

LV torsion is twist normalized to the distance between the apex and base (degrees/cm) (Fig. 12.25).

Table 12.6 Brief review of some clinical implications of parameters of LV mechanics

Estimation of LV filling pressures	Average E/e' ≥14 is correlated with elevated LV filling pressure [24]
Detection of subclinical diseases/ early myocardial involvement	Reduction in strain/strain rate may occur before changes in LVEF in systemic hypertension, diabetes mellitus, systemic sclerosis or lupus Erythematosus amyloidosis, muscular dystrophy, or changes in LV function after cancer treatment [6, 25–27]
Constrictive vs. restrictive physiology	In the absence of myocardial disease, e' velocities typically remain normal in constrictive pericarditis (usually >8 cm/s). Deformation (longitudinal and radial) are impaired in RCM and the GCS may remain normal. In CP, only circumferential strain shows abnormalities [28, 29]
Athlete's heart vs. HCM	The reduced e' velocities could be in favor of HCM [30]
	Subjects with HCM had lower global longitudinal strain but higher dispersion when compared with hypertensive LVH [6]
Myocardial ischemia	Reduction in strain by 2D STE more objective and accurate than assessment of WMA
	Longitudinal, radial, and circumferential strain reduced in ischemic areas in coronary artery disease
	Post-systolic thickening (deformation), detected by radial strain correlates with the severity of ischemia
Myocardial infarction	Global peak systolic strain rate -0.9 S^{-1} are highly sensitive and specific for the identification of patients with prior myocardial infarction
	2D STE successful in differentiating transmural from subendocardial infarction by showing lower circumferential strain in the former
	Decreased LV segmental longitudinal strain predicts progressive LV dilatation after myocardial infarction
Myocardial viability	Strain measurements by 2D STE more objective and accurate than visual WMA for assessment of myocardial viability during low-dose dobutamine stress echocardiography
	2D STE differentiates active contraction from passive motion due to tethering
Cardiac resynchronization therapy (CRT)	Combining longitudinal strain from TDI velocity with 2D STE radial strain may help in predicting response to CRT
	Longitudinal strain delay index (calculated from the difference between peak and endsystolic strain) of >25% predicts response to CRT (sensitivity 95%, specificity 83%)
	Speckle Tracking and Resynchronization (STAR) study showed that radial and transversal strain were better than longitudinal and circumferential strain in predicting
	LVEF response and long-term survival after CRT
	Lack of dyssynchrony before CRT by 2D STE radial strain associated with death or hospitalization for heart failure
Valvular heart disease	Decreased radial, circumferential, and longitudinal strain in patients with severe aortic stenosis and normal LVEF. Long-term follow-up after valve replacement showed significant improvement with no change in EF
	Reduced preoperative 2D STE longitudinal strain in the ventricular septum (apical four-chamber view) predicts a postoperative LVEF decrease of ≥10% in patients with chronic severe mitral regurgitation
Congenital heart disease	Atrial septal defect—basal clockwise rotation during systole is reduced
	Tetralogy of Fallot—right ventricular global longitudinal strain and strain rate is decreased significantly
Detection of rejection and coronary stenosis in heart transplant patients	Sudden reduction of ≥15% in global radial strain associated with acute rejection
	Decrease in strain and strain rate at rest and with dobutamine stress echo also useful to detect significant coronary stenosis

Normal Rotation values in young adults are shown in Table 12.7.

LV torsion is a sensitive marker to assess impaired LV function, which has many clinical implications.

Apical rotation has been proved to be an indicator of myocardial ischemia, heart failure with preserved EF, hypertrophic cardiomyopathy, and valvular heart disease. In mitral regurgitation, torsion and untwisting usually normal when EF is normal, and decrease with decline in systolic function. It remains to be seen whether the changes in LV torsion can help determine the timing of surgical repair.

In early stages of cardiac amyloidosis, amyloid proteins are deposited in the subendocardium. Accordingly, longitudinal deformation is reduced but circumferential deformation is preserved. Twist and untwisting are normal. With advanced disease, circumferential deformation is affected and peak twist and untwisting rate are reduced [15] (Figs. 12.26, 12.27, and 12.28).

In Table 12.8, some of the clinical implication of twist/untwist have been shown.

Despite the growing evidence in support of clinical implications of LV twist measurements using 2D STE, routine clinical use of this methodology is not recommended at this time [6].

Fig. 12.25 Apical rotation in degrees of rotation (*y* axis) vs. time in seconds (*x* axis). Notice the presence of an initial small clockwise rotation (deflection below baseline, followed by counterclockwise rotation. Basal rotation in degrees (*y* axis) vs. time (*x* axis). Notice the presence of an initial small counterclockwise rotation (deflection above baseline), followed by clockwise rotation
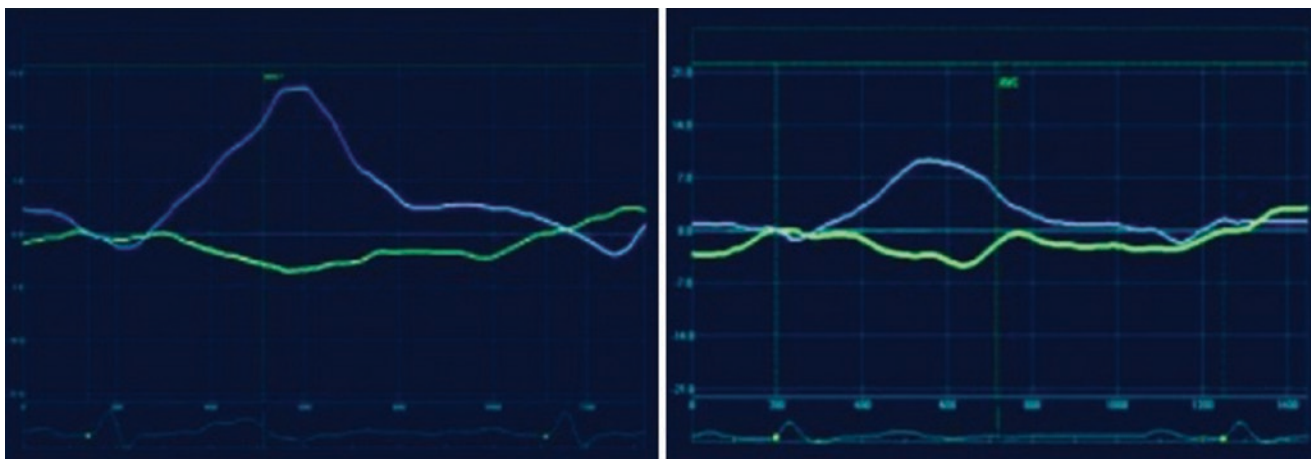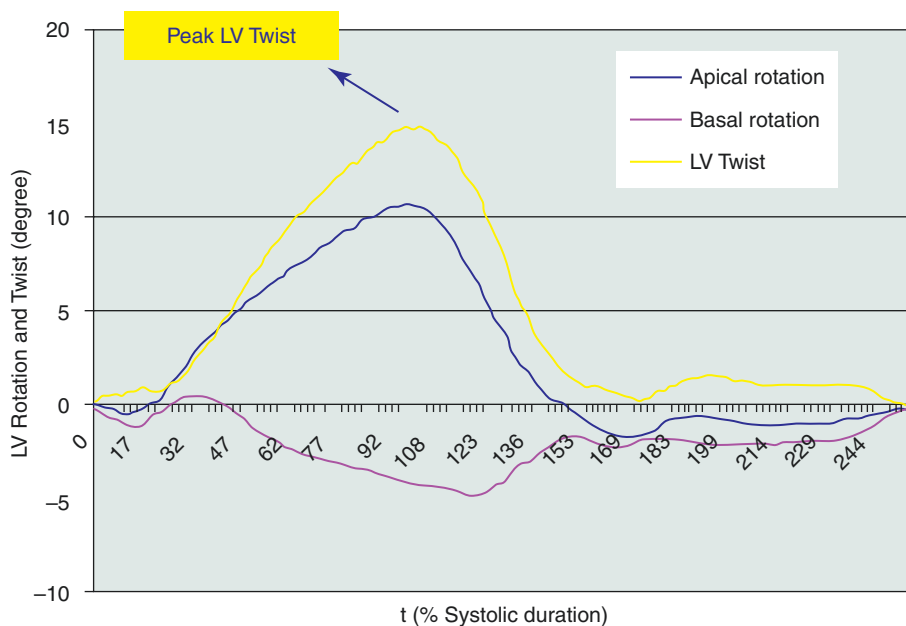
Fig. 12.26 Significantly reduced apical rotation in DCM patient (right panel) in compared with normal subject (left panel). There is no important difference in basal rotation between two cases

Table 12.7 Normal values for parameters of rotation

Parameter	Mean ± SD
Peak apical rotation (°)	10.1 ± 1.9
Peak apical rotation rate (°/s)	61.6 ± 25.3
Peak basal rotation (°)	4.9 ± 2
Peak basal rotation rate (°/s)	44.2 ± 17.8

Modified table from Reproduced from Takahashi K, Al Naami G, Thompson R. Normal rotational, torsion and untwisting data in children, adolescents and young adults. J Am Soc Echocardiogr. 2010;23:286–93

Right Ventricle

DTI and STE both provide indices of RV function. DTI (Pulsed wave and color- coded) allows quantitative assessment of RV systolic and diastolic longitudinal motion (Fig. 12.29) by means of measurement of myocardial velocities from the apical four- chamber view.

DTI of tricuspid annulus provides assessment of systolic (systolic velocity) and diastolic function (Early and late diastolic velocities and the ratio of tricuspid inflow early velocity to early diastolic annulus velocity).

Isovolumic myocardial acceleration (IVA; calculated by dividing the maximal isovolumic myocardial velocity by the time to peak velocity; unit: m/s^2) have also been used for assessment of RV systolic function (less affected by RV shape or loading conditions compared to Systolic velocity) [34] (Fig. 12.30).

At the level of the tricuspid annulus, in the RV free wall, normal systolic velocity by pulsed DTI is >12 cm/s. A peak systolic velocity <10 cm/s should raise the suspicion of abnormal RV function, especially in younger adults [35]. Another parameter of RV function is right ventricular index

Fig. 12.27 Reverse apical rotation (clock-wise) in end-stage DCM patient with significant fibrotic tissue
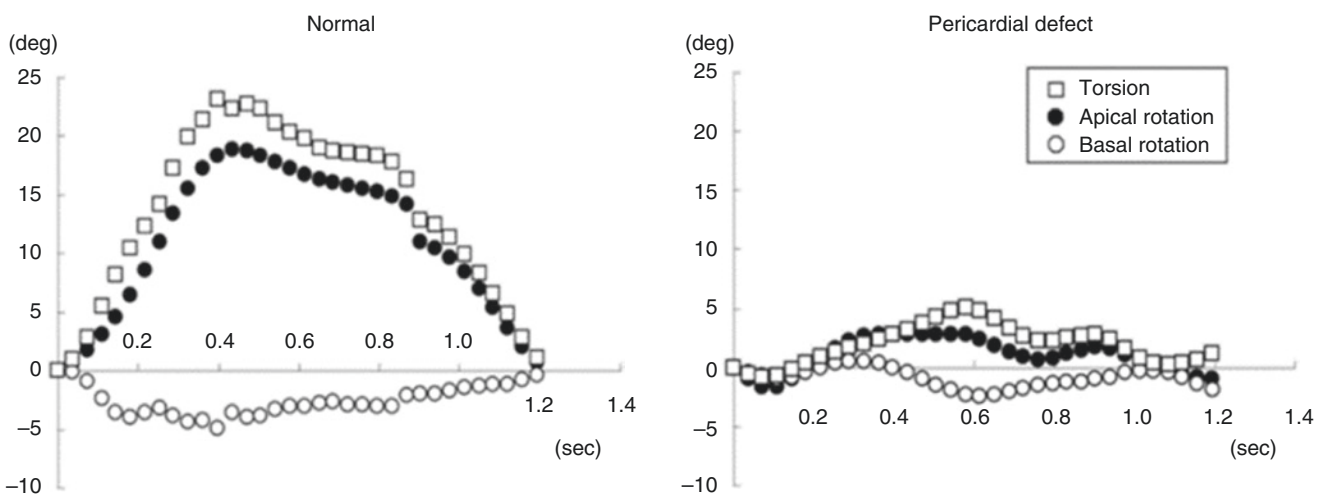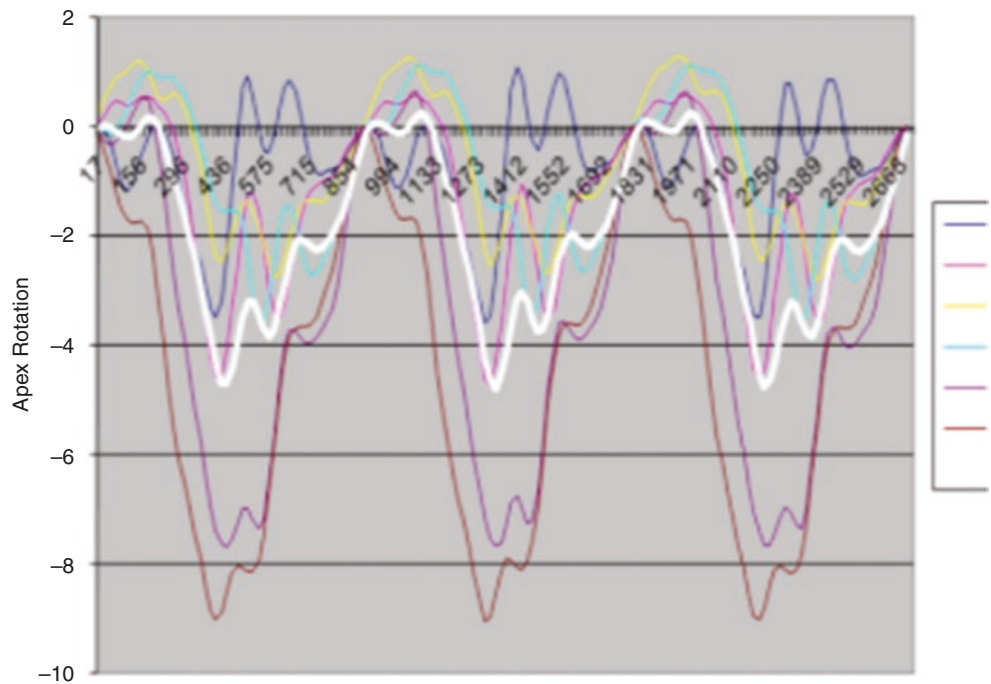
Fig. 12.28 Lack of Twist in patient constrictive Pericarditis

of myocardial performance (RIMP). It is an index of global RV performance. The isovolumic contraction time, the isovolumic relaxation time, and ejection time intervals should be measured in a same cycle (Fig. 12.31). RIMP >0.54 denotes to RV dysfunction. In conditions with elevated RA pressures, RIMP can be falsely low (due to probable association with IVRT shortening).

In healthy individuals, RV longitudinal velocities demonstrate a typical base-to-apex gradient with higher velocities at the base (Fig. 12.32) as in LV. With RV dysfunction, RV longitudinal velocities decrease and the base-to-apex gradient tends to disappear.

In addition, RV velocities are consistently higher compared with the left ventricle. This can be explained by the differences in loading conditions and compliance with a lower afterload in the right ventricle and the dominance of longitudinal and oblique myocardial fibers in the RV free wall [6].

Table 12.8 LV twist in different pathologies

	LV Twist	Untwisting	Time to peak untwisting
Heart failure			
With preserved LVEF	→ or ↑	→ or ↑	Delayed
With reduced LVEF	↓	↓	Delayed
Coronary artery disease			
Subendocardial MI	→	→	Delayed
Transmural MI	↓	↓	Delayed
LV hypertrophy			
Hypertension	→ or ↑	↓	Delayed
HCM	Variable	Variable	Delayed
Aortic stenosis	↓	→ or ↑	Delayed
Dilated cardiomyopathy	↓	↓	Delayed
Pericardial disease	↓	↓	No data
Restrictive CMP	↓[a]	↓[a]	No data

HCM hypertrophic cardiomyopathy, *MI*, myocardial infarction; ↓ reduced;, ↑ elevated; → unchanged

Modified table from: Mor-Avi V, Lang RM, Badano LP, Belohlavek M, Cardim NM, Derumeaux G, Galderisi M, Marwick T, Nagueh SF, et al. Current and Evolving Echocardiographic Techniques for the Quantitative Evaluation of Cardiac Mechanics: ASE/EAE Consensus Statement on Methodology and Indications Endorsed by the Japanese Society of Echocardiography. Eur J Echocardiogr. 2011;12:167–205

[a]In RCM, the subendocardial fiber dysfunction will be associated with depressed GLS and GRS, whereas the spared epicardial fibers will lead to normal or increased GCS, left ventricular (LV) torsion, and LV torsional rate. With disease progression the torsion/torsion rate will decrease
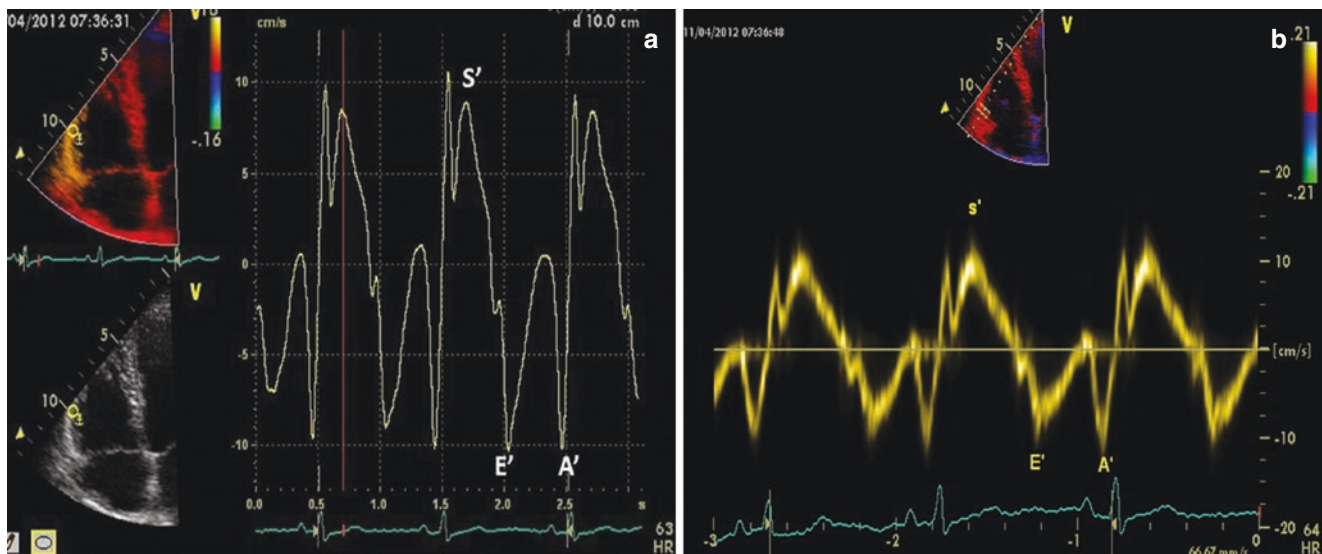
Fig. 12.29 Right ventricle Myocardial velocity, provided by Color Doppler (**a**) and Spectral Doppler (**b**). S′ denotes to systolic velocity and E′ and A′ are related to the diastolic phase

Myocardial Deformation

In RV, like LV, Strain/strain rate imaging could be used for assessment of myocardial function (Figs. 12.33 and 12.34).

In the right ventricle, there is a reverse base-to-apex gradient, reaching the highest values in the apex.

Cutoff points of systolic strain and SR at the basal RV free wall of −25% and −4 s⁻¹ with sensitivities of 81 and 85% and specificities of 82% and 88%, respectively, to predict RV EF >50% [6].

In patients with RV disease or dysfunction, peak systolic strain and SR are significantly reduced and delayed compared

Fig. 12.30 The velocity waveform obtained from color Doppler of RV free wall (with ROI in the basal part). IVA (red line) is measured as isovolumic contraction wave rises from zero line, reaching to its peak point
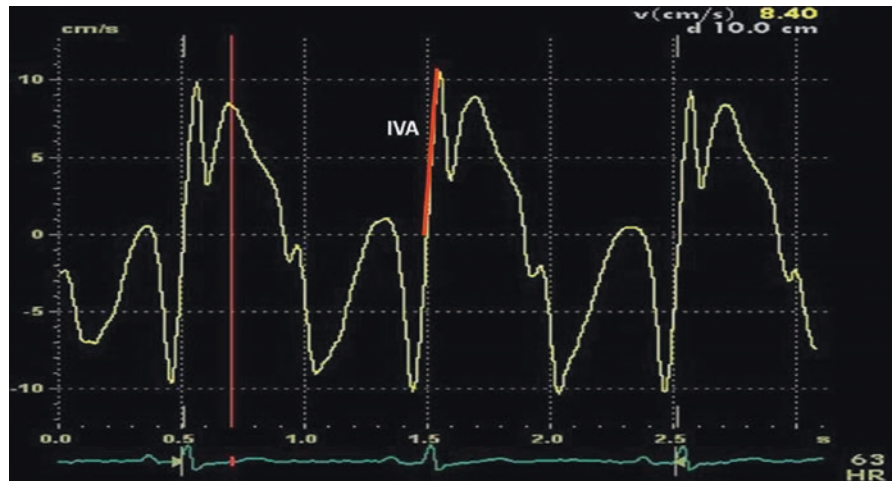

Fig. 12.31 Spectral Doppler of tricupsid annulus, used for measurement of RV MPI ((IVCT + IVRT/ET) which was about 0.45 in this case
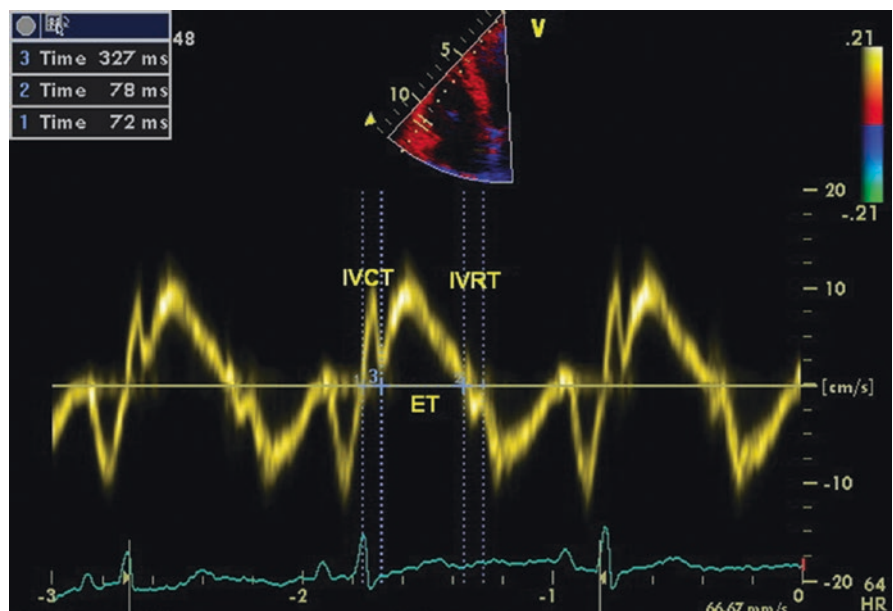
Fig. 12.32 Color coded DTI for assessment of RV myocardial velocity, showing a base to apex gradient
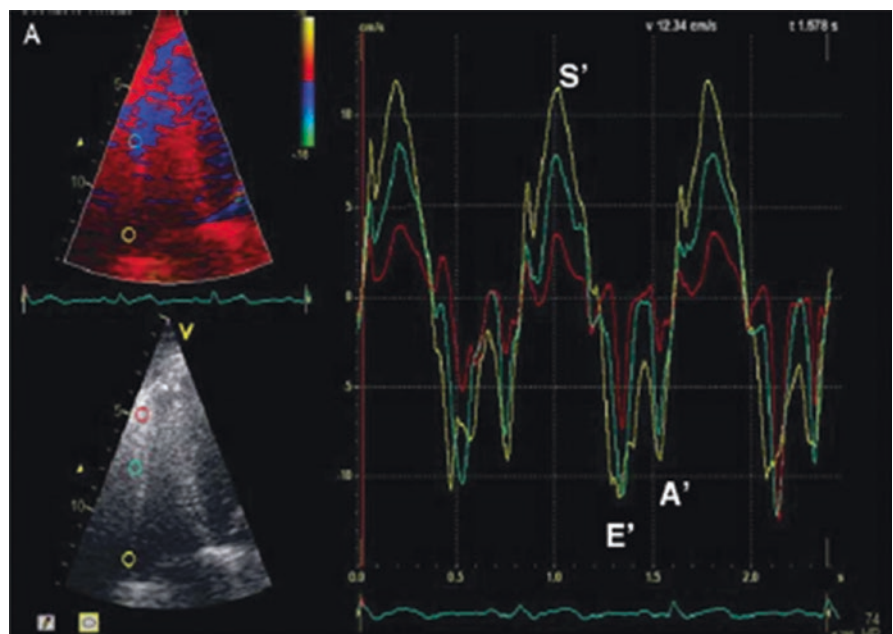
Fig. 12.33 Strain Analysis of RV by Tissue Doppler derived Strain (**a**) and 2d–STE (**b**). In panel b, global strain as average of strain in RV free wall and the septum has been provided (−22%)
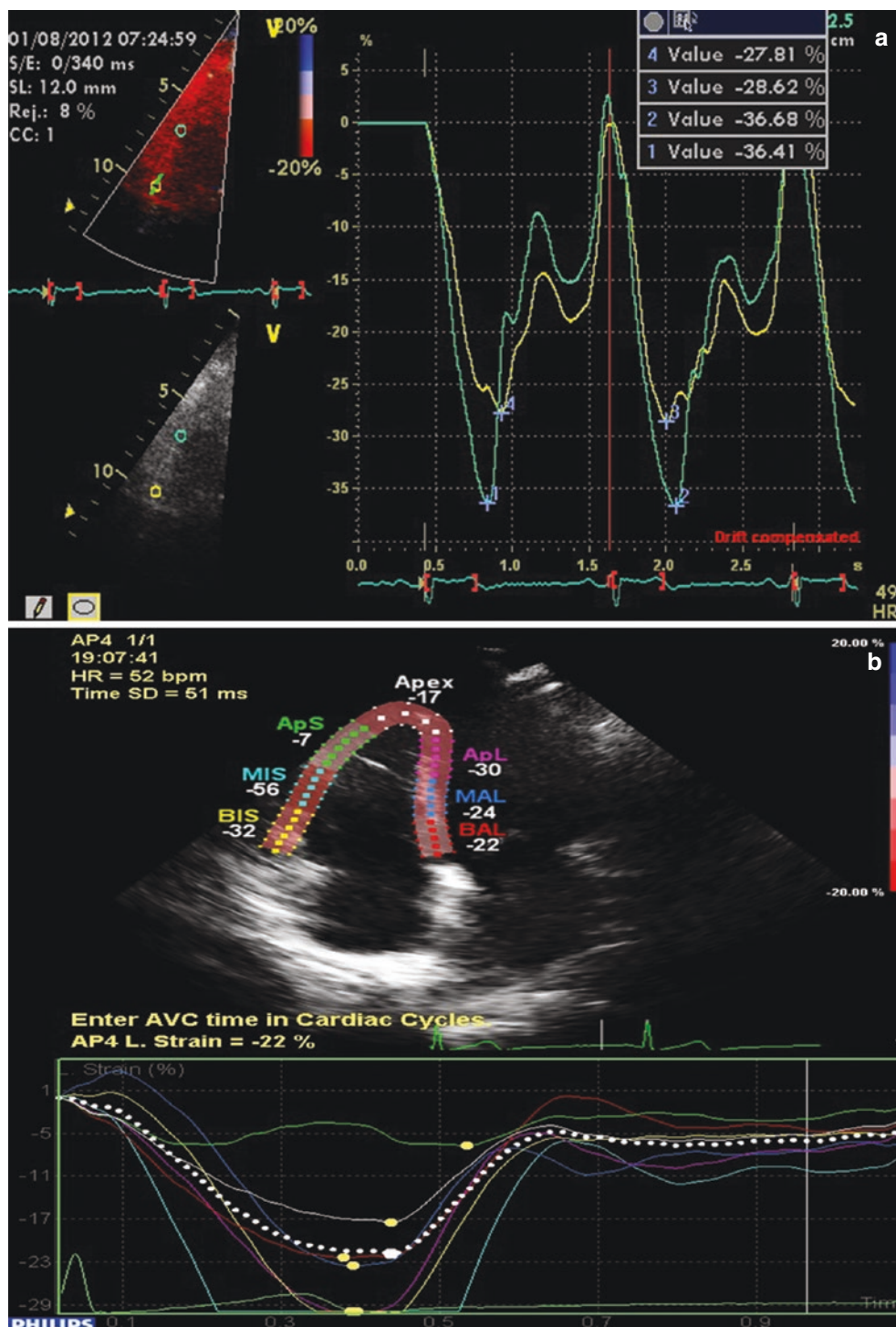

with healthy normal. Normal values of multiple parameters of RV function are presented in Table 12.9.

Left Atrium

Myocardial imaging can be used to evaluate left atrial (LA) function. Both DTI and 2D -STE allow noninvasive assessment of global and regional LA function [6]. The mitral annulus late diastolic velocity is easy to measure, has a high reproducibility. It can be affected by LA contractility as well as LA afterload [36]. 2d–STE successfully provides LA volume curves during one cardiac cycle, from which various LA mechanical indices can be obtained [37–42].

The first (total of 12 equidistant regions, six in the apical four-chamber view and six in the apical two-chamber view) takes as a reference point the QRS onset and measures the positive peak atrial longitudinal strain (corresponding to
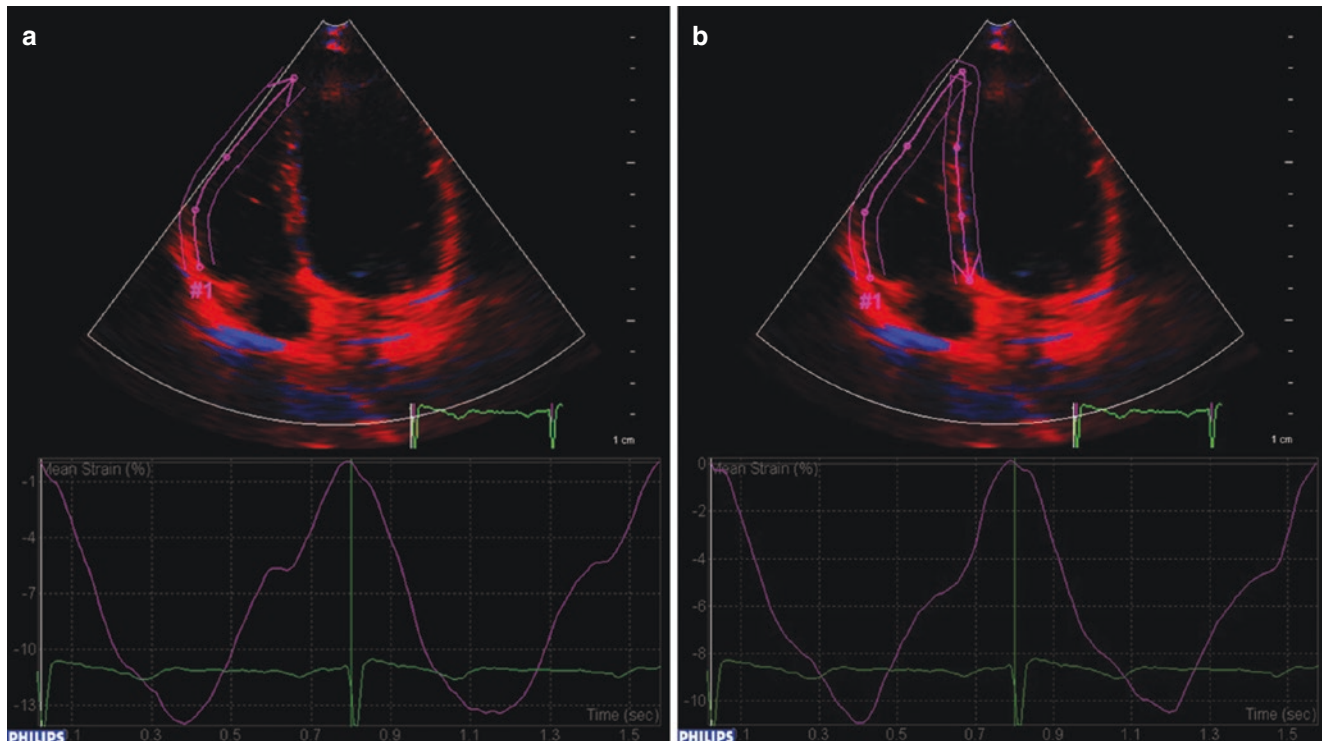
Fig. 12.34 Mean strain in RV free wall and RV free wall + septum (using SQ application)

Table 12.9 Normal values for DTI and 2D–STE related parameters of RV function

Parameter	Mean ± SD	Abnormality threshold
Pulsed Doppler S wave (cm/s)	14.1 ± 2.3	<9.5
Color Doppler S wave	9.7 ± 1.85	<6.0
RV free wall 2D strain (%)	−29 ± 4.5	Cut off point: −20
Tissue Doppler MPI	0.38 ± 0.08	>0.54
E′/A′	1.18 ± 0.33	<0.52
E′	14.0 ± 3.1	<7.8
E/E′	4.0 ± 1.0	>6.0

Modified table from Lang RM, Badano LP, Mor-Avi V, Afilalo J, Armstrong A, Ernande L, Flachskampf FA, et al. Recommendations for Cardiac Chamber Quantification by Echocardiography in Adults: An Update from the American Society of Echocardiography and the European Association of Cardiovascular Imaging. J Am Soc Echocardiogr. 2015;28:1–39

atrial reservoir) [37–41]. The mean peak atrial longitudinal strain was 42.2 ± 6.1% (Fig. 12.35).

The second (total of 15 equidistant regions, six in the apical four-chamber view, six in the apical two- chamber view, and three in the inferoposterior wall in long axis) uses the P wave as the reference point, enabling the measurement of a first negative peak atrial longitudinal strain (corresponding to atrial systole), a second positive peak atrial strain (corresponding to LA conduit function), and their sum [37, 39–44] (Fig. 12.28b).

The average values of positive and negative peak strain were 23.2 ± 6.7% and 14.6 ± 3.5%, respectively.

Utility of LA strain in daily practice is still limited. It has been used in those of atrial fibrillation to predict maintenance of sinus rhythm after cardioversion.

Right Atrium

Similar to left atrium, RA have a passive and active phase of contraction which could be a target for assessment. But clearly there is no validated data on RA strain measurement in such a way that to be considered for routine clinical use [37, 39–41, 45–47] (Figs. 12.36 and 12.37).
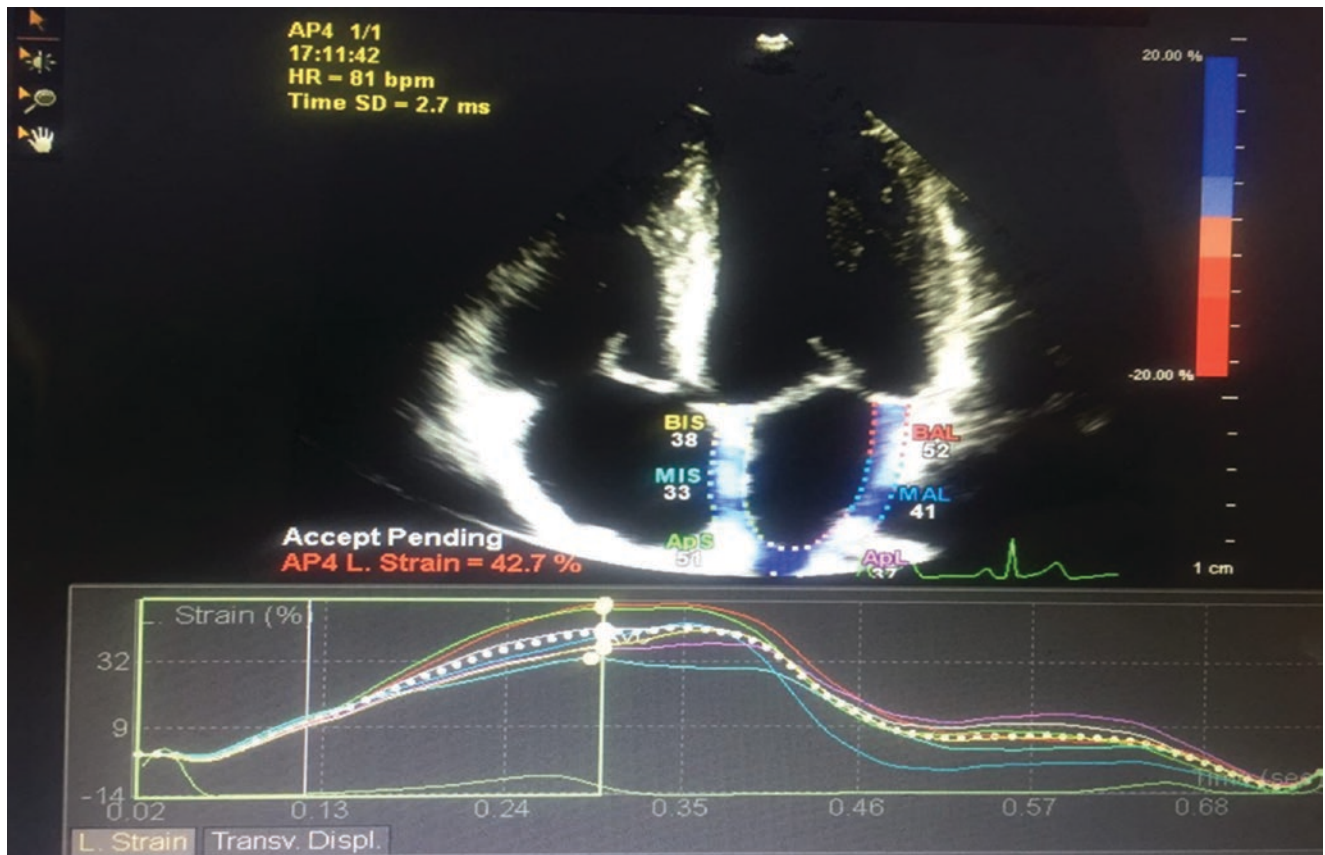
Fig. 12.35 Global and longitudinal LA strain four chamber apical view (with QRS as the reference point)
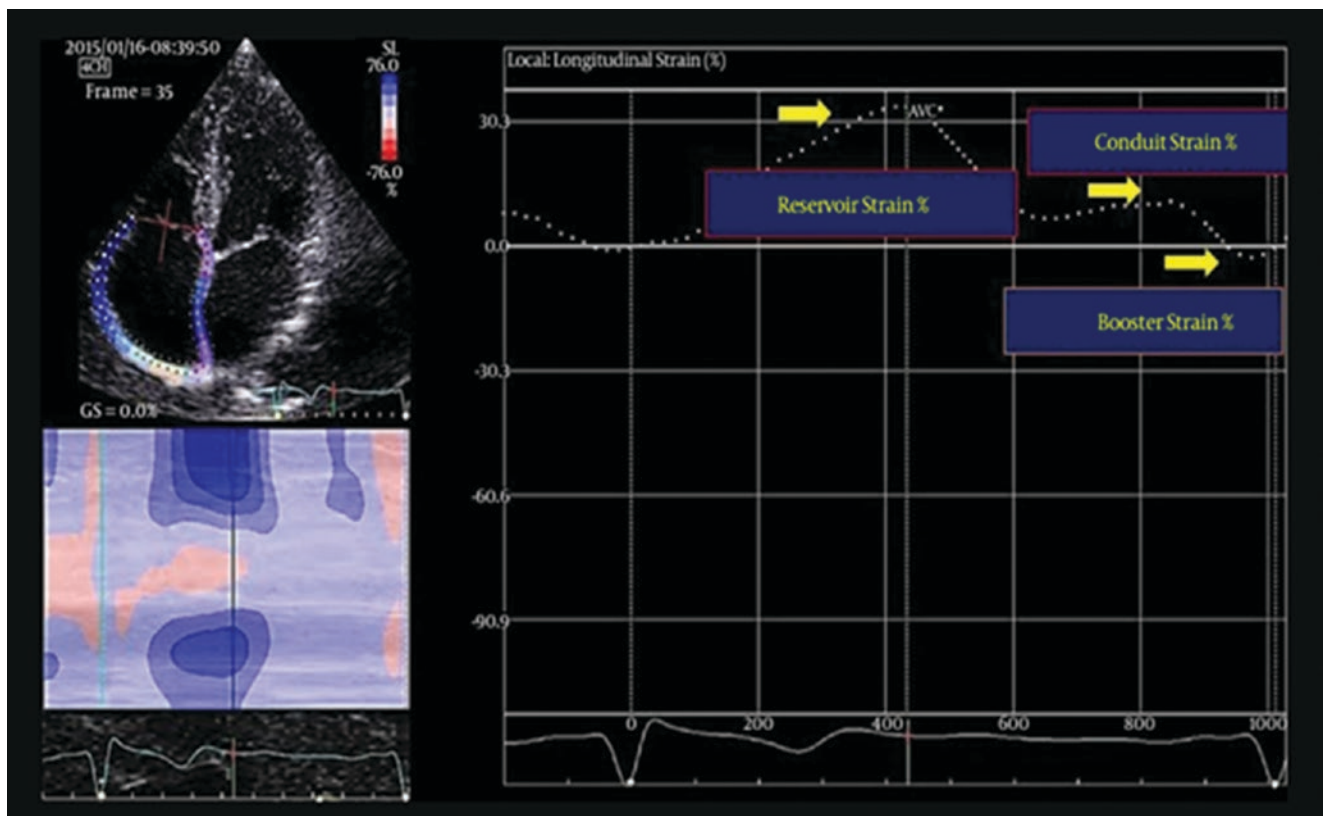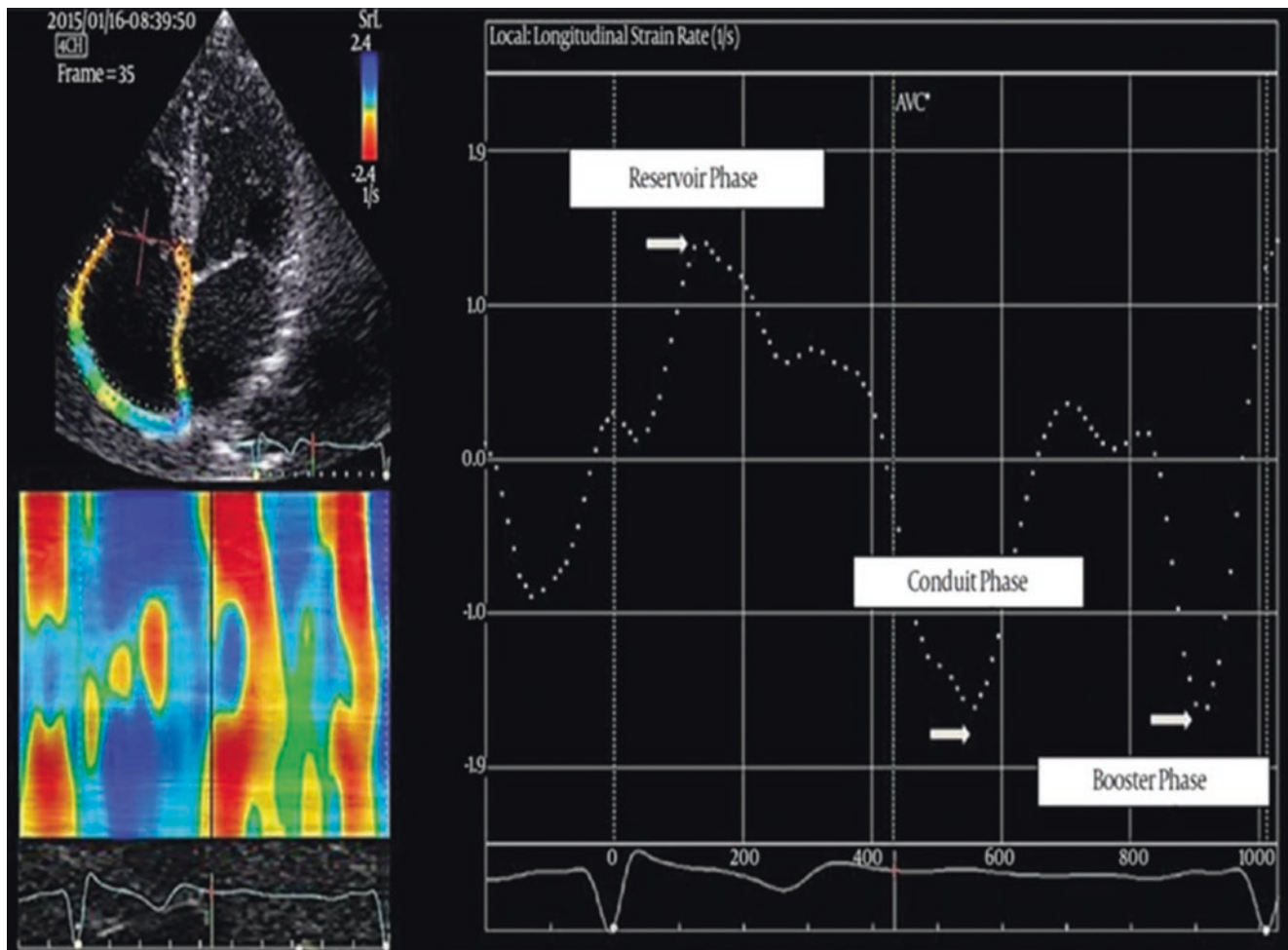

Fig. 12.36 Right atrial strain (%) imaging, showing three mechanical phases in a normal subject

Fig. 12.37 Right atrial strain rate imaging, showing three mechanical phases in a normal subject

Conclusion

DTI and STE and tortional parameters provided objective diagnostic tools in cardiac mechanics. Although their use have been expanded in daily practice, standardization is needed for both the method of measurement and also among the different vendors. On the other hand, additional testing are still necessary to validate the data of parameters of myocardial function [6, 45–51].

Questions

1. All the following statements are the advantages of 2D-Specke tracking (relative to the tissue Doppler imaging) except:
   A. Better Temporal Resolution
   B. Angle Independency
   C. Not influenced by translational motion
   D. Better spatial resolution

2. Which parameter of LV mechanics does not change in constrictive pericarditis?
   A. Longitudinal strain
   B. Circumferential strain
   C. Twisting
   D. Untwisting

3. All following changes could result in optimization of the images in Color Coded DTI, except:
   A. Reducing sector width
   B. Increasing Depth
   C. Gain adjustment
   D. Optimize gray scale display

4. Which one of the following statements is correct about Spectral Pulsed Doppler:
   A. It has excellent temporal resolution.
   B. Mean velocities at a given site could be achieved.
   C. Multiple segments can be examined at a time.
   D. Gain setting has no effect on the results.

5. Which type of strain could be obtained in apical long-axis views:
   A. Radial strain
   B. Circumferential strain
   C. Transverse strain
   D. Shear strain

Answers

1. A
   2d-STE had lower frame rate and poor temporal resolution. Consequently, it has limited utility in tachycardia or non-sinus rhythm)

2. B
   In CP, circumferential strain is reduced but both longitudinal and radial strain are not affected. In RCM, longitudinal, radial are reduced and circumferential strain might be preserved.

3. B
   Narrow sector and reduced depth result in higher frame rate and better images.

4. A
   In spectral Doppler (in contrast to color DTI), peak velocities could be obtained. Excessive gain should be avoided, because can result in over-estimating the velocities. Only one segment can be examined at a time.

5. C
   Transverse strain-, though it is the changes in myocardial thickness- needs long axis apical views.

References

1. Kostis JB, Mavrogeorgis E, Slater A, et al. Use of a range gated, pulsed ultrasonic Doppler technique for continuous measurement of velocity of the posterior heart wall. Chest. 1972;62(5):597–604.
2. McDicken WN, Sutherland GR, Moran CM, et al. Colour Doppler velocity imaging of the myocardium. Ultrasound Med Biol. 1992;18(6–7):651–4.
3. Miyatake K, Yamagishi M, Tanaka N, et al. New method for evaluating left ventricular wall motion by color-coded tissue Doppler imaging: in vitro and in vivo studies. J Am Coll Cardiol. 1995;25(3):717–24.
4. Geyer H, Caracciolo G, Abe H, et al. Assessment of myocardial mechanics using speckle tracking echocardiography: fundamentals and clinical applications. J Am Soc Echocardiogr. 2010;23(4):351–69.
5. Notomi Y, Setser RM, Shiota T, et al. Assessment of left ventricular torsional deformation by Doppler tissue imaging: validation study with tagged magnetic resonance imaging. Circulation. 2005;111:1141–7.
6. Mor-Avi V, Lang RM, Badano LP, Belohlavek M, Cardim NM, Derumeaux G, Galderisi M, Marwick T, Nagueh SF, et al. Current and evolving echocardiographic techniques for the quantitative evaluation of cardiac mechanics: ASE/EAE consensus statement on methodology and indications endorsed by the Japanese Society of Echocardiography. Eur J Echocardiogr. 2011;12:167–205.
7. Otto CM. Advanced echocardiographic modalities. In: Textbook of clinical echocardiography. 5th ed. Philadelphia, PA: Elsevier Saunders; 2013. p. 98–103.
8. Sutherland GR, Bijnens B, McDicken WN. Tissue Doppler echocardiography: historical perspective and technological considerations. Echocardiography. 1999;16(5):445–53.
9. Abraham TP, Dimaano VL, Liang HY. Role of tissue Doppler and strain echocardiography in current clinical practice. Circulation. 2007;116:2597–609.
10. Gilman G, Khandheria BK, Hagen ME, et al. Strain rate and strain: a step-by-step approach to image and data acquisition. J Am Soc Echocardiogr. 2004;17:1011–20.
11. D'Hooge J, Heimdal A, Jamal F, et al. Regional strain and strain rate measurements by cardiac ultrasound: principles, implementation and limitations. Eur J Echocardiogr. 2000;1:154–70.
12. Lang RM, Goldstein SA, Kronzon I, Khandheria BK, Mor-Avi V. ASE's comprehensive echocardiography. 2nd ed. Philadelphia, PA: Elsevier Saunders; 2016. p. 13–6.
13. Heimdal A, Stoylen A, Torp H, Skjaerpe T. Real-time strain rate imaging of the left ventricle by ultrasound. J Am Soc Echocardiogr. 1998;11:1013–9.
14. Urheim S, Edvardsen T, Torp H, Angelsen B, Smiseth OA. Myocardial strain by Doppler echocardiography. Validation of a new method to quantify regional myocardial function. Circulation. 2000;102:1158–64.
15. Gillam LD, Otto CM. Advanced approaches in echocardiography. Philadelphia, PA: Elsevier Saunders; 2012. p. 84–114.
16. Brown J, Jenkins C, Marwick TH. Use of myocardial strain to assess global left ventricular function: a comparison with cardiac magnetic resonance and 3-dimensional echocardiography. Am Heart J. 2009;157:102–5.
17. Amundsen BH, Helle-Valle T, Edvardsen T, Torp H, Crosby J, Lyseggen E, et al. Noninvasive myocardial strain measurement by speckle tracking echocardiography validation against sonomicrometry and tagged magnetic resonance imaging. J Am Coll Cardiol. 2006;47:789–93.
18. Biswas M, Sudhakar S, Nanda NC, Buckberg G, Prradhan M, Roomi AU, et al. Two- and three-dimensional speckle tracking echocardiography: clinical applications and future directions. Echocardiography. 2013;30(1):88–105.
19. Gjesdal O, Hopp E, Vartdal T, Lunde K, Helle-Valle T, Aakhus S, et al. Global longitudinal strain measured by two-dimensional speckle tracking echocardiography is closely related to myocardial

infarct size in chronic ischaemic heart disease. Clin Sci (Lond). 2007;113:287–96.

20. Nesser HJ, Mor-Avi V, Gorissen W, Weinert L, Steringer-Mascherbauer R, Niel J, et al. Quantification of left ventricular volumes using three- dimensional echocardiographic speckle tracking: comparison with MRI. Eur Heart J. 2009;30:1565–73.

21. Maffessanti F, Nesser HJ, Weinert L, Steringer-Mascherbauer R, Niel J, Gorissen W, et al. Quantitative evaluation of regional left ventricular function using three-dimensional speckle tracking echocardiography in patients with and without heart disease. Am J Cardiol. 2009;104:1755–62.

22. Kuznetsova T, Herbots L, Richart T, D'hooge J, Thijs L, Fagard RH, et al. Left ventricular strain and strain rate in a general population. Eur Heart J. 2008;29:2014–23.

23. Lang RM, Badano LP, Mor-Avi V, Afilalo J, Armstrong A, Ernande L, Flachskampf FA, et al. Recommendations for cardiac chamber quantification by echocardiography in adults: an update from the American Society of Echocardiography and the European Association of Cardiovascular Imaging. J Am Soc Echocardiogr. 2015;28:1–39.

24. Nagueh SF, Smiseth OA, Appleton CP, Byrd BF, Dokainish H, Edvardsen T, et al. Recommendations for the Evaluation of left ventricular diastolic function by echocardiography: An update from the American Society of Echocardiography and the European Association of Cardiovascular Imaging. J Am Soc Echocardiogr. 2016;29:277–314.

25. Marwick TH. Measurement of strain and strain rate by echocardiography ready for prime time? J Am Coll Cardiol. 2006;47: 1313–27.

26. Jurcut R, Wildiers H, Ganame J, D'hooge J, De BJ, Denys H, et al. Strain rate imaging detects early cardiac effects of pegylated liposomal Doxoru- bicin as adjuvant therapy in elderly patients with breast cancer. J Am Soc Echocardiogr. 2008;21:1283–9.

27. Poorzand H, Mirfeizi SZ, Javanbakht A, Alimi H. Comparison of echocardiographic variables between systemic lupus erythematosus patients and a control group. Arch Cardiovasc Imag. 2015;3(2):eee30009.

28. Sengupta PP, Mohan JC, Mehta V, Arora R, Pandian NG, Khandheria BK. Accuracy and pitfalls of early diastolic motion of the mitral annulus for diagnosing constrictive pericarditis by tissue Doppler imaging. Am J Cardiol. 2004;93:886–90.

29. Claus P, Salem Omar AM, Pedrizzetti G, Sengupta PP, Nagel E. Tissue tracking technology for assessing cardiac mechanics principles, normal values, and clinical applications. J Am Coll Cardiol Img. 2015;8:1444–60.

30. Cardim N, Oliveira AG, Longo S, Ferreira T, Pereira A, Reis RP, et al. Doppler tissue imaging: regional myocardial function in hypertrophic cardiomyopathy and in athlete's heart. J Am Soc Echocardiogr. 2003;16:223–32.

31. Narula J, Vannan M, DeMaria AN. Of that waltz in my heart. JACC. 2007;49:917–20.

32. Notomi Y, Lysyansky P, Setser RM, et al. Measurement of ventricular torsion by two-dimensional ultrasound speckle tracking imaging. J Am Coll Cardiol. 2005;45:2034–41.

33. Nanda NC. Comprehensive textbook of echocardiography. New Delhi: Jaypee Brothers Medical Publishers; 2014, p.363.

34. Tigen MK, Karaahmet T, Gurel E, Dundar C, Pala S, Cevik C, Akcakoyun M, Basaran Y. The role of isovolumic acceleration in predicting subclinical right and left ventricular systolic dysfunction in hypertensive obese patients. Turk Kardiyol Dern Ars. 2011;39(1):9–15.

35. Rudski LG, Lai WW, Afilalo J, Hua L, Handschumacher M, Chandrasekaran K, et al. Guidelines for the echocardiographic assessment of the right heart in adults: a report from the

American Society of Echocardiography. J Am Soc Echocardiogr. 2010;23:685–713.

36. Nagueh SF, Sun H, Kopelen HA, et al. Hemodynamic determinants of the mitral annulus diastolic velocities by tissue Doppler. J Am Coll Cardiol. 2001;37:278–85.

37. Saraiva RM, Demirkol S, Buakhamsri A, Greenberg N, Popovic ZB, Thomas JD, et al. Left atrial strain measured by two-dimensional speckle tracking represents a new tool to evaluate left atrial function. J Am Soc Echocardiogr. 2010;23:172–80.

38. Cameli M, Caputo M, Mondillo S, Ballo P, Palmerini E, Lisi M, et al. Feasibility and reference values of left atrial longitudinal strain imaging by two-dimensional speckle tracking. Cardiovasc Ultrasound. 2009;7:6.

39. Ojaghi Z, Alizadehasl A, Maleki M, Naderi N, Esmaeilzadeh M, Noohi F, Azarfarin R. Echocardiographic assessment of right atrium deformation indices in healthy young subjects. Arch Cardiovasc Imaging. 2013;1(1):2–7.

40. Ojaghi-Haghighi Z, Alizadehasl A, Hashemi A. Reverse left ventricular apical rotation in dilated cardiomyopathy. Arch Cardiovasc Imaging. 2015;3(2):e28112.

41. Naderi N, Ojaghi Z, Pezeshki S, Alizadehasl A. Quantitative assessment of right atrial function by strain imaging in adult patients with totally corrected tetralogy of fallot. Arch Cardiovasc Imaging. 2013;1(1):8–12.

42. Sadeghpour A. Incremental value of left atrium two-dimensional strain in patients with heart failure. Arch Cardiovasc Image. 2013;1(2):49–50. https://doi.org/10.5812/acvi.15896.

43. Ojaghi Haghighi Z, Mostafavi A, Anita S, Peighambari MM, Alizadehasl A, Moladoust H, Ojaghi Haghighi H. Echocardiographic assessment of left ventricular twisting and untwisting rate in normal subjects by tissue Doppler and velocity vector imaging: comparison of two methods. Arch Cardiovasc Imaging. 2013;1(2):63–71. https://doi.org/10.5812/acvi.14289.

44. Zahra Ojaghi Haghighi S, Alizadehasl A, Ardeshiri M, Peighambari MM, Moladust H, Sameie N, et al. The torsional parameters in patients with nonischemic dilated cardiomyopathy. Arch Cardiovasc Imaging. 2015;3(1):e26751. https://doi.org/10.5812/acvi.26751.

45. Alizadehasl A, Sadeghpour A, Hali RR, Bakhshandeh H, Badano L. Assessment of left and right ventricular rotational interdependence: a speckle tracking echocardiographic study. Echocardiogr J. 2017;34(3):415–21.

46. Saha SK. Pulmonary arterial hypertension: a two-dimensional echocardiographic approach from screening to prognosis. Arch Cardiovasc Imaging. 2016;4(2):e41818. https://doi.org/10.5812/acvi.41818.

47. Mihaila S, Cucchini U, Marzaro A, Muraru D, Andras K, Altiok E, Vinereanu D, Sadeghpour A, Alizadehasl A, Badano LP, Becker M. Fully automated measurements of left atrial volume are highly feasible and accurate compared to expert manual measurements: a comparative multi-center study using a novel automated analysis algorithm. In: Abstract presentation. ESC; 2017.

48. Salehi R, Alizadehasl A. Tissue Doppler imaging values in hypertrophic cardiomyopathy according to left ventricular outflow gradient. J Cardiovasc Thorac Res. 2011;2(4):19–22.

49. Alizadehasl A, Haghighi SZO, Sadeghpour A, Bezanjani FN. Echocardiographic assessment of left ventricle torsional parameters by tissue Doppler and velocity vector imaging: comparison of the two Methods. J Am Coll Cardiol. 2013;1(2):63–71.

50. Alizadehasl A, Azarfarin R. Tissue Doppler imaging findings including Prominent S wave in patients with mitral valve prolapse. Arch Cardiovasc Imaging. 2014;1(3):e17123.

51. Kyavar M, Sadeghpour A, Hashemi A, Alizadehasl A, Sanati HR, Hashemi A. The prognostic value of mitral annulus velocities by

tissue Doppler imaging after first anterolateral myocardial infarction. Iranian Heart J. 2013;13(4):(Scopus).

52. Voigt JU, Lindenmeier G, Exner B, Regenfus M, Werner D, Reulbach U, Nixdorff U, Flachskampf FA, Daniel WG. Incidence and characteristics of segmental postsystolic longitudinal shortening in normal, acutely ischemic, and scarred myocardium. J Am Soc Echocardiogr. 2003;16(5):415–423.

53. Manish B, Ravi R. Kasliwal. How do I do it? Speckle-tracking echocardiography. Indian Heart J. 2013;165:117–23.

54. Blessberger H, Binder T. Non-invasive imaging: two dimensional speckle tracking echocardiography: basic principles. Heart. 2010;96:716–722.